Quaternary Science Reviews 214 (2019) 68–86

Contents lists available at ScienceDirect

Quaternary Science Reviews

journal homepage: www.elsevier.com/locate/quascirev

Holocene sea-level database for the Rhine-Meuse Delta, The Netherlands: Implications for the pre-8.2 ka sea-level jump

Marc P. Hijma [a, *], Kim M. Cohen [b, a]

[a] Deltares Research Institute, Dept. of Applied Geology and Geophysics, Utrecht, the Netherlands
[b] Utrecht University, Dept. of Physical Geography, Utrecht, the Netherlands

ARTICLE INFO

Article history:
Received 24 December 2017
Received in revised form
10 April 2019
Accepted 1 May 2019

Keywords:
Holocene
Sea-level changes
Europe
Netherlands
Radiogenic isotopes
Sea-level jump
Rhine-Meuse

ABSTRACT

This paper provides the most-accurate sea-level index points (SLIPs) for the Rhine-Meuse Delta (RMD), The Netherlands, identified amidst a wealth of data accumulated in sixty years of research. Following documented protocols, 106 selected radiocarbon dates from peat beds from transgressed valley floor, upper estuarine and back-barrier lagoonal settings were first listed individually, then screened in ensemble on quantified age-depth position and inshore palaeotidal setting. The database contains 50 SLIPs and 56 upper limiting data points spanning a depth range of −34 to −1.5 m. The dates in the database originate from dedicated sea-level research, which kept surface elevation and sampling depth uncertainty small, and sampling of basal-peat beds was favoured, keeping compaction uncertainties small too.

The SLIPs cover an age-range of 8.8–3.0 ka BP and are available from Greater Rotterdam and its near offshore. For upper limiting data points, the coverage extends offshore, tracing the Rhine palaeovalley, and reaches back to 11.5 ka BP. The age-depth data density and spatial concentration of subsets of dates allow to perform Bayesian radiocarbon calibration and to reduce temporal uncertainty by 25% for the average sample (1σ age uncertainty ≈ 75 cal. yr), when depth position and rates of relative sea-level rise (RSLR) are used to assign sequence order. Between 8.0–4.5 ka BP, rates of RSLR gradually decreased from 9 to 1 mm/yr. In the millennium before, rates of RSLR were much higher, on average 10 mm/yr, and marked by a sea-level jump between 8.45–8.2 ka BP. A two-phased nature of this jump starts to be resolved, with local magnitudes of 1.7 ± 0.6 m (1σ, first phase) and 0.2 ± 0.2 m (second phase), corresponding to globally-averaged jumps of 2.5 m ± 0.9 m for the first and 0.3 ± 0.3 m for the second phase. For the pre-9 ka BP period, only offshore upper limiting data points are currently available. Until new offshore data are gathered, trends of RSLR before 9 ka BP can only be estimated, fed with global insights in post-glacial eustasy, regional estimates regarding rates of glacio-isostatic adjustments and tectonic subsidence, and sedimentary geological interpretations of scattered basal-peat presence.

1. Introduction

Large parts of The Netherlands are part of a sedimentary depocentre within the tectonically subsiding North Sea Basin (Kooi et al., 1998). The largest river system into this basin is that of the Rhine-Meuse, which in response to Holocene sea-level rise formed the back-barrier Rhine-Meuse Delta (RMD) in the western Netherlands (Berendsen and Stouthamer, 2000). The RMD is positioned over the Rhine-Meuse palaeovalley (Fig. 1) that formed in the Last Glacial Maximum, a time when the basin floor in the study area was temporarily upwarped as part of glacio-isostatic adjustment (GIA), owing to its proximity to Fennoscandian and British ice sheets to the northeast and northwest (Kiden et al., 2002; Vink et al., 2007). The palaeovalley ran along the southern flank of the joint peripheral forebulge crest of these ice masses (Busschers et al., 2007). In deglacial and postglacial times, forebulge collapse amplified rates of subsidence in the study area while it was inundated by the rising sea. Because of the considerably increased subsidence, rates of relative sea-level rise (RSLR) in the area were faster in the first half of the Holocene than in most other shelf regions, and hence rapid transgression of the river valleys and interfluves of the North Sea low lands occurred.

* Corresponding author.
E-mail address: marc.hijma@deltares.nl (M.P. Hijma).

https://doi.org/10.1016/j.quascirev.2019.05.001
0277-3791/

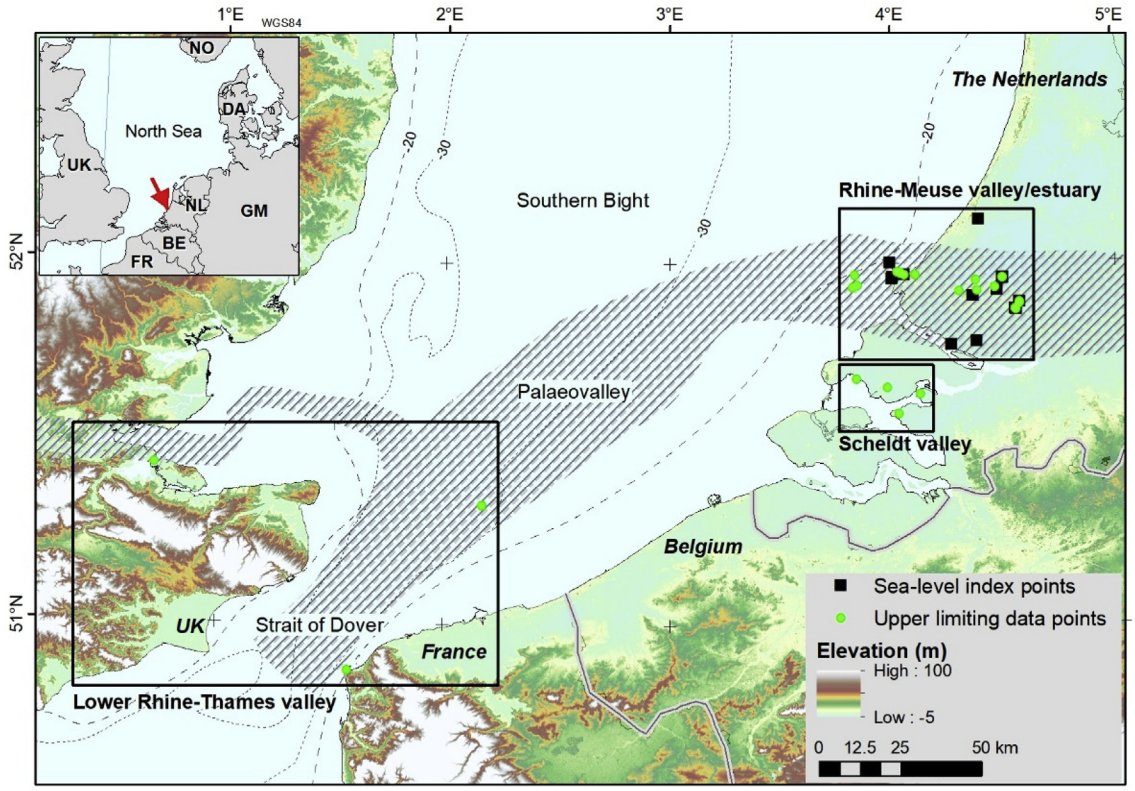

Fig. 1. Overview of the locations of the sea-level data points in the database and a hatched Last Glacial Maximum Rhine-Meuse-Thames palaeovalley (based on Hijma et al., 2012). Abundant data from within the Rhine-Meuse valley/estuary (red arrow in inset map), is supplemented with a few data points from the Lower Rhine-Thames and Scheldt valleys to track earlier Holocene transgression of the combined offshore valley. (For interpretation of the references to colour in this figure legend, the reader is referred to the Web version of this article.)

Abundant sediment supply from the river Rhine stimulated the development of thick sequences of alternating fine-grained and organic deposits from upper estuarine and lower deltaic interdistributary swamp and marsh settings. Peat beds from such environments, that encroached over sloping palaeosurfaces, offer an excellent opportunity for working up samples to index points of sea-level change (SLIPs). In the RMD these sequences have been intensively studied over the last decades, resulting in 1) robust relative sea-level (RSL) reconstructions, resulting in the longest and densest RSLR-dataset of The Netherlands (e.g. Van de Plassche et al., 2010), 2) detection of accentuated accelerations in RSLR, e.g. the 8.45–8.2 ka BP sea-level jump (Hijma and Cohen, 2010) and 3) an important contribution to the development of sea-level research methodologies (Van de Plassche, 1986). The sea-level data from The Netherlands, however, is at present not available in the contained form of a standardized database that can be used for further research, incorporated in global databases, and be publicly scientifically maintained. Furthermore, the steadily accumulated data have not yet been uniformly categorized in terms of precision and suitability. To clarify: protocols to address precision and suitability have been developed and applied in earlier studies that compiled datasets for the RMD and wider Netherlands' surroundings (notably Van de Plassche, 1982; Kiden, 1995; Kiden et al., 2002; Vink et al., 2007; Hijma and Cohen, 2010; Koster et al., 2017), but these differ, for example, between multi-site compilations (categorization of scattered individual samples) and studies concentrating on densely vertically sampled single localities (categorization of a sample based on neighbours in series). The goal of this paper is to provide a screened list of the most accurate SLIPs for the RMD, stored in a geological sea-level database format compliant to that of the whole special issue, using a protocol that by design would also be applicable to other transgressed valley and deltaic settings for which legacy RSL-data are to be screened. These settings contain many subenvironments, though, and when one wants to obtain high-quality series of SLIPs from them, it is necessary to understand the evolution of the deltaic wedge and its shifting subenvironments as a whole (Vis et al., 2015). This was already illustrated in the classic Middle Holocene RMD sea-level reconstructions from the 1960–80 period (Jelgersma, 1961; Van de Plassche, 1982; Roep and Beets, 1988; Van de Plassche and Roep, 1989). A much larger density of sea-level data for the RMD has accumulated since, from new sites and because classic sites were resampled and redated with improved methods, which occurred while geological mapping resolution increased and while palaeoenvironmental understanding improved. This has led to revision and extensions of the RSL data and derived sea-level curves for the RMD.

In this paper we list and assess the full body of RSL-relevant basal-peat samples that currently exists in the RMD and palaeovalley literature. The main body of data is from the lower RMD (Rotterdam and surroundings) and covers 8.8–3.0 ka BP (all ages in this paper are in calibrated years BP, i.e. before 1950 CE). Earlier phases of transgression affected the downstream continuation of the palaeovalley offshore towards the Strait of Dover (Fig. 1), a far less intensively sampled area from which data points are of lesser quality (producing upper limiting points rather than SLIPs). The paper screens both the inshore and the offshore subsets, to demonstrate the applied procedures and outcomes (database quality), and to deliver data overview that in addition to use in regional and global sea-level rise studies is also relevant for

documenting 'valley transgression' and 'river base-level forcing' (for which sea-level data provides the observational control). The paper does not cover geological sea-level data from other parts of The Netherlands, although a comparable wealth of data exists for these regions (see Meijles et al., 2018 for a recent example). Further dedicated efforts are needed to include also these data into a geological sea-level database as in this paper, to make it cover all sectors of the Dutch coast (also advocated in Vermeersen et al., 2018) and to allow updates of studies on regional differences in GIA (e.g. Van de Plassche, 1982; Kiden, 1995; Kiden et al., 2002; Vink et al., 2007; Koster et al., 2017; Meijles et al., 2018).

To define the relevance of a data point to RSL reconstruction, the well-established concept of indicative meaning, introduced in the 1980s (Van de Plassche, 1986) and most recently described in the Handbook of Sea-Level Research (Shennan et al., 2015), is applied. The data-screening procedures in this paper stepwise establish the indicative meaning of each sample considered, stored over a series of fields (columns) in the database. The procedure first considers the indicative meaning of samples individually to establish age-depth data points with quantified uncertainty boxes, and then in further steps evaluates their positions amongst neighbouring samples in age-depth data series. The second step extends beyond evaluating data series from individual sites and uniform environmental settings (2D evaluation) to include comparison between sites from adjacent palaeoenvironments (3D/4D evaluation). This is necessary because within back-barrier systems and drowned wide valleys, inland tidal and fluvial effects may influence the vertical precision of SLIPs. In the RMD such effects became known from 1) variations observed in SLIPs between sites (Van de Plassche, 1995; Berendsen et al., 2007; Van de Plassche et al., 2010) and 2) insights in the operation of tides in inlets and estuaries, and flood basins (e.g. Zonneveld, 1960; Van der Woude, 1984; Van Veen et al., 2005; Vis et al., 2015; De Haas et al., 2018).

In the following sections of the paper, we introduce the sea-level research sites of the RMD, describe the contents of the database and present the RSL reconstructions that it produces. We explicitly address our categorization of the samples, distinguish SLIPs from upper limiting data points, and outline the specific sea-level research concepts for transgressed-valley and back-barrier deltaic settings on which these distinctions are based. The results are discussed on aspects of 1) comparison with previous published reconstructions for the RMD, 2) new insights into the 8.45–8.2 ka BP sea-level jump, and 3) transgression of the Rhine-Meuse palaeovalley offshore between the Strait of Dover and The Netherlands.

2. Regional setting and history of sea-level research in the Rhine-Meuse Delta

The RMD is commonly labelled as a back-barrier delta, and the region used to harvest data for sea-level reconstruction its lower delta plain. During the marine transgression (in the Early and Middle Holocene prior to coastal-barrier establishment), the palaeovalley transformed into a broad, low-shouldered estuary with a back-stepping bay-head delta complex marking the inland transgression limit. Coeval with barrier-system establishment, the bay-head delta began prograding and avulsions started, completing the evolution from valley to estuary to back-barrier delta (Hijma and Cohen, 2011a). Below we describe the peats that have been used for RSL reconstructions.

2.1. Peat beds on inland dune flanks

At several places, Late-Glacial to Early Holocene inland aeolian-dune fields are part of the buried palaeovalley topography, with locally much more accentuated substrate relief than the palaeovalley floodplain and its cover sand rims provide. These inland dune fields have dune flanks and tops, rising meters above the palaeosurface surroundings. During Holocene RSLR, first the lower parts and later on the higher parts of these dunes were buried with deltaic deposits: swampy fen peat at times when these sites happened to be distal from active fluvial-tidal channels, and with more clayey deposits at times when they were proximal. It is these sites that were targeted intensively in the sea-level reconstruction field campaigns of Jelgersma (1961) and Van de Plassche (1982) and following work (Berendsen et al., 2007; Van de Plassche et al., 2010), as well as by archaeologists (Louwe Kooijmans, 1974; Louwe Kooijmans et al., 2005), and fluvial geomorphologists-sedimentologists tracing the influence of rising sea level on ground-water levels (GWLs) and sedimentary conditions in the inland delta plain (Van Dijk et al., 1991; Törnqvist et al., 1998; Cohen, 2005; Koster et al., 2017; Van Asselen et al., 2017).

The reason to target these aeolian-dune sites was that it allowed collecting vertical series of basal-peat samples that would be minimally affected by compaction, and across such a small area that regional differential subsidence problems would be circumvented. In addition, because the dunes stood out as islands in the flood basins, the water depth in which the fen peat beds formed on their flanks could be relatively well constrained (set to 0.1 m, see next sections). The isolation of the inland dune sites as small sandy islands in otherwise marshy and swampy flood basins also circumvented certain regional groundwater-hydrological effects on water tables at the time the peat encroached the dune flank. This makes these central-delta sites more suitable than samples obtained from along the flanks of the palaeovalley (De Vries, 1974; Van de Plassche, 1982; Cohen, 2005).

The above advantages are the reason that vertical series of dates obtained from the base of the dune-flank basal peat were targeted as indicators of water-level rise, with care taken not to sample underlying organic palaeosol A-horizons and to remove rootlets from higher up (Van de Plassche, 1982), or to pick specific terrestrial macrofossils (Berendsen et al., 2007; Van de Plassche et al., 2010). Working with samples from the base of the peat bed (and not from the centre or the top of the peat) further minimized compaction-related uncertainties. Repeated resampling and redating, including switching from conventional ^{14}C dating of bulk samples to Accelerator Mass Spectrometry (AMS) ^{14}C dating of picked botanical macrofossils (Törnqvist et al., 1998; Berendsen et al., 2007; Van de Plassche et al., 2010), have confirmed the consistency of the age-depth relationships in the series of basal-peat samples from individual sites and the region at large.

For constructing a continuous record of RSLR between 7.5–3 ka BP, SLIPs from several dune sites in the Lower RMD have been combined (e.g. from Hillegersberg to Vlaardingen to Bolnes-Barendrecht; Fig. 2). A sea-level curve is generally tied to the dune sites from which the index points plot lowest, hereby assuming that these index points formed in an area that had the most-suppressed tidal and river gradients during the time period of interest (see next sections), and hence at a back-barrier water level (governing peat formation) closest to contemporary mean sea level (MSL, Van de Plassche, 1995; Van de Plassche et al., 2010).

For the post-3 ka BP period, human occupation and extensive activities in the delta plain (drainage, embankment, creation of 'polders', artificially lowering of water tables, peaty top soil oxidation) have destroyed natural-depositional archives in the back-barrier area. This means that RSL reconstructions for the Late Holocene have to rely on methods other than basal-peat dates (Roep and Beets, 1988; Van de Plassche and Roep, 1989; De Groot et al., 1996).

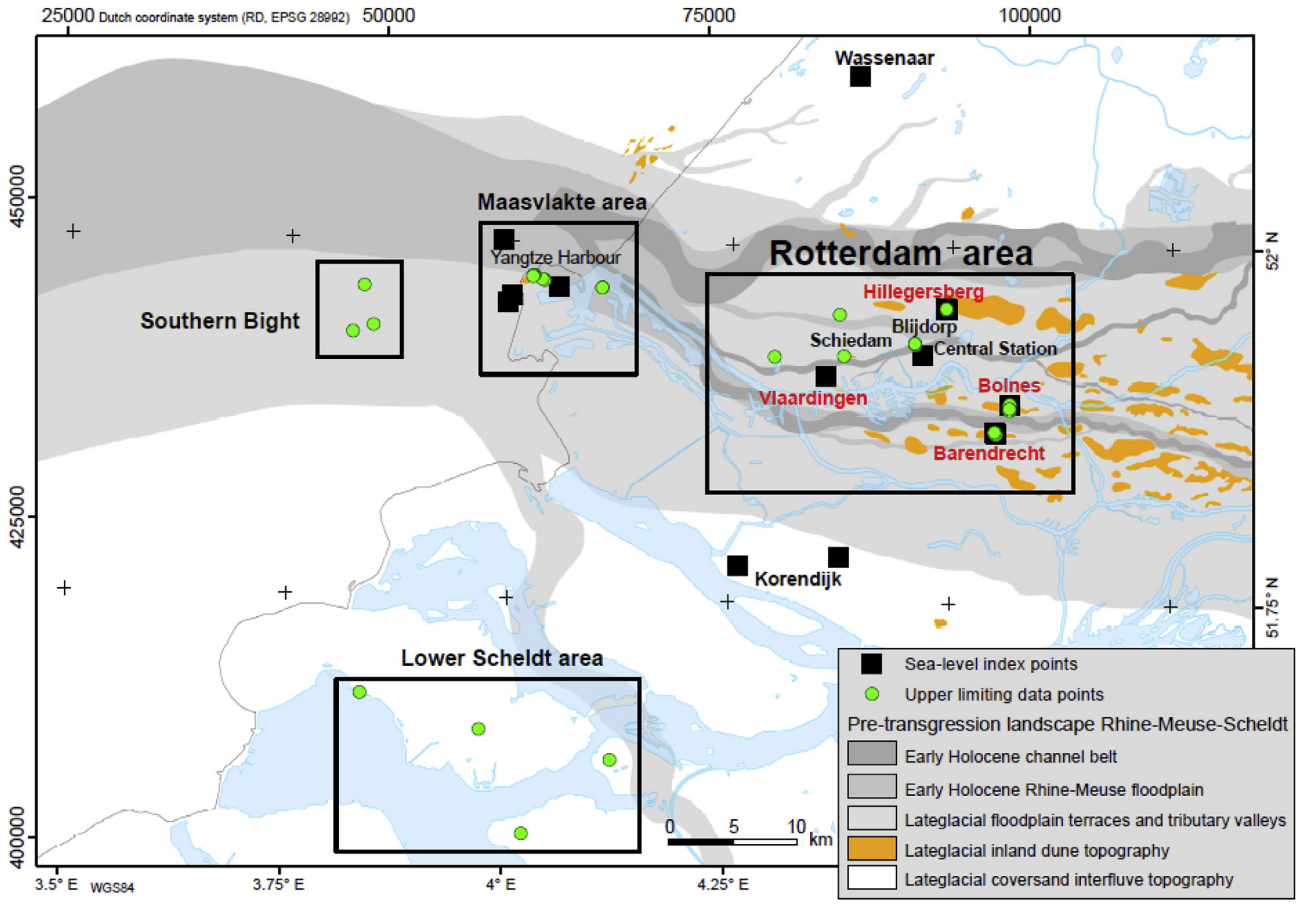

Fig. 2. Location of RSL reconstruction sites in the Rhine-Meuse delta included in the database, and their regional grouping. The Rotterdam area holds most of the data. The names of the inland aeolian-dune sites that were used by Jelgersma and Van de Plassche are written in red. Palaeovalley outline and distribution of cover sand and dunes fields are based on Hijma et al. (2012), Cohen et al. (2012) and Cohen et al. (2017). (For interpretation of the references to colour in this figure legend, the reader is referred to the Web version of this article.)

2.2. Peat beds in the palaeovalley

For the pre-7.5 ka BP period, the inland dunes in the Rotterdam area (Figs. 2 and 3) are, for cumulative reasons, less suitable for sea-level reconstructions. The dunes used for RSL research are high dunes with steep flanks, but near their base the dune-foot topography commonly, if not always, flattens into an extensive meter-thick blanket of sandy aeolian facies connecting to surrounding dunes, and grades into clayey floodplain facies of Early Holocene age (Hijma et al., 2009; Vos et al., 2015). Basal peats covering the dune foot and floodplain clays have been sampled and this dataset is meaningful to Early Holocene sea-level rise and hence included in our database. Because they come from settings and positions, they are less favourable for direct (unfiltered) use as RSL data points than basal peats sampled higher-up on the isolated dune, and the arguments to assign certain samples SLIP status will differ for dune flank and dune-foot-and-valley-floor settings (section 3.7). Furthermore, a vertical gap exists in occurrence of peats along the lower most parts of the Rotterdam. Swamp environments that formed extensive basal-peat beds were absent between ~8.5 and 8 ka BP – the period that the Rotterdam area was actually transgressed – whereas instead subaqueous organic and clayey facies (gyttja, clay-gyttja, humic clays) were mostly deposited, with only locally some discontinuous peat formation (Cohen, 2005; Hijma and Cohen, 2010). Sedimentological and palynological records show that the rate of water-table rise was too fast for peat formation by organic production to keep up. For producing a pre-7.5 ka BP sea-level curve it is therefore necessary to use data from sites relatively further apart.

Basal-peat data from 9.0-8.5 ka BP comes from the densely studied Maasvlakte area (Figs. 2 and 3; Hijma and Cohen, 2010, 2011a). As in more upstream regions, large fields of aeolian landforms are present (Hijma et al., 2010; Vos et al., 2015). North Sea transgressive activity, however, has been of higher energetic nature in the downstream open marine and outer estuarine regimes, which in the Maasvlakte area has truncated the dune tops rather than burying them. Only over former dune foot areas, have basal peats locally survived erosion. Along the southern side of the palaeovalley (Fig. 2), such dune-foot basal peats were found between 21 and 19 m below O.D. and have been dated (Vos et al., 2015) as part of geoarchaeological investigation of the Mesolithic site 'Yangtzehaven'. Seismic data of the seabed along the northern side of the palaeovalley (Hijma et al., 2010) show relatively low and partly truncated aeolian dunes at levels between 19 m and 16 m below O.D. (Figs. 2 and 3). These dunes seem extensively capped by, presently undated, peat beds.

The pre-7.5 ka BP basal peat also exists extensively in offshore and inshore parts of the Rhine-Meuse valley floor, away from dune forms and dune-foot blankets. Botanic composition and clay admixture shows the valley-floor peats to commonly represent fluvial flood basin swamp-environments that established over floodplain clays of Early Holocene and Late Glacial age (Hijma et al.,

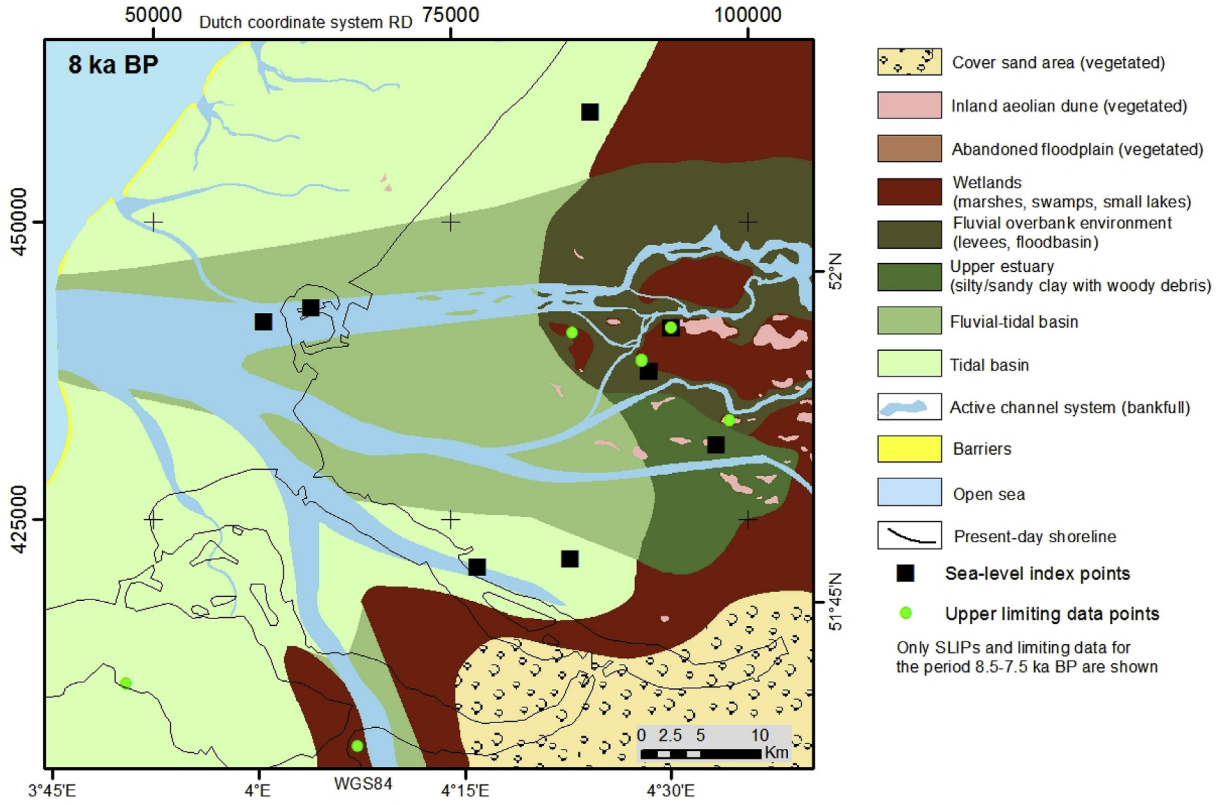

Fig. 3. Palaeogeographical map for ~8 ka BP (modified from Hijma and Cohen, 2011a) with locations of 8.5–7.5 ka BP data points. Such maps are available at ~0.5 kyr intervals (Hijma and Cohen, 2011a; Vos et al., 2011) and have been used to place the sampled sea-level indicators in their palaeoenvironmental context.

2009). These floodplain clays are stiff and show palaeosol features from subaerial exposure prior to being overlain by peat. Hence, the vertical accuracy of index points derived from valley-floor basal-peats is not majorly substrate-compaction affected (Cohen, 2005; Koster et al., 2017). The larger contributor to uncertainty in RSL reconstruction is the variation in indicative meanings that exists within these sites, compared to sites on the toes and flanks of dune forms.

On the valley floor, the peat-producing swamps maintained gently sloping groundwater tables, graded to the feeding fluvial system and to run-off from seepage-fed tributaries coming from the palaeovalley rims. At a given longitudinal position in the palaeovalley, basal peats that started to form relatively early would have formed meters above sea level at the time of formation, while other basal peats, at very similar depths but of younger ages, can have formed only decimeters above sea level. Indeed, where valley floor basal peats are densely sampled, considerable scatter exists in dated onsets of basal-peat formation (Cohen, 2005; Koster et al., 2017). To overcome the issues with using valley-floor basal-peat beds in RSL reconstruction, sampling activity has focused on describing and dating the top of the basal-peat beds. At a good number of coring sites, the basal peat is non-erosively overlain by (brackish) fluvial-tidal flood-basin deposits and in such cases the top of the peat bed can be used (full relevance for sea-level reconstruction). A downfall of making use of samples from the top of basal-peat beds is that the compaction-related uncertainty increases with the bed thickness. But when basal peats are just centimeters to a decimeter thick in their compacted state, dating its top still provides for a superior SLIP, since at that thickness uncertainty about the amount of compaction for a top-of-peat sample is smaller than the scatter observed in the less favourable base-of-peat. If the peat bed is thicker, however, top-of-peat SLIPs have larger compaction uncertainties. In that case, they are not by default superior to base-of-peat data points in the same age-depth positions.

To summarise the above: basal-peat beds from various settings within the Rhine-Meuse delta have been sampled and dated and used for GWL and RSL reconstructions. A selection of samples from bases of peat beds on dune flanks and from tops of peat beds on valley floors and dune toes can be categorized as 'SLIPs', and the remainder 'upper limiting data points'.

3. Holocene relative sea-level database for the Rhine-Meuse Delta, The Netherlands

The database (accessible via the data repository) contains a selected 106 ^{14}C dates from the various basal-peat beds in the RMD, which after screening categorize as 50 SLIPs and 56 upper limiting data points. The selection restricted itself to samples centimeters to decimeters above a consolidated substrate (for low compaction uncertainty) and from relatively seaward geographic positions (the lower delta and offshore). Basal peats from further inland carry little additional information to RSL reconstruction and are excluded due to the uncertainties that river-gradient effects introduce (discussed in section 3.7). Radiocarbon dates from other abundant types of indicators, including molluscs and charcoal within archaeological contexts, have also been excluded. There is considerable vertical uncertainty with respect to their indicative meaning and in the RMD they carry little additional RSL information.

The majority of the selection is from the Rotterdam area, with important sample series derived from the dune sites Barendrecht, Bolnes, Hillegersberg and Vlaardingen (Jelgersma, 1961; Van de

Plassche, 1982, 1995; Berendsen et al., 2007; Van de Plassche et al., 2010) and from temporal outcrops in open construction pits (Hijma et al., 2009; Hijma and Cohen, 2010). In addition, we have included previously unreleased data from the Rotterdam area. From the offshore Maasvlakte area we have incorporated the data of Van Heteren et al. (2002), Hijma and Cohen (2010), Vos (1992), Vos et al. (2010), Vos (2013), Vos and Cohen (2014) and Vos et al. (2015). A few pre-8 ka BP data points are available from the Scheldt palaeovalley in the vicinity of its confluence with the Rhine-Meuse system (Jelgersma, 1961; Kiden, 1995; Slupik et al., 2014). The oldest data points in the database come from farthest offshore, from the submerged Rhine-Thames confluence reach of the palaeovalley through the Strait of Dover (Fig. 1; Morzadec-Kerfourn and Delibrias, 1972; Kirby and Oele, 1975; Devoy, 1979).

The content of the database is described in the next sections. The order of presentation resembles a workflow of first retrieving information from original sources, then processing the data to document positions, ages and uncertainties uniformly, then screening and identifying the SLIPs among the entries.

3.1. Geographic location

The position of all onshore data points was originally measured, either by leveling or using a GPS-system, and reported using the Dutch coordinate system (Rijksdriehoekstelsel, EPSG: 28992). Coordinates were converted to decimal degrees (WGS-1984) and rounded to four decimals, meaning that a point can be located within ~10 m. The older data points of Jelgersma (1961) were rounded to three decimals since their coordinates have larger uncertainties according to Berendsen et al. (2007). The offshore data points were originally reported in either UTM or WGS coordinates and have been converted to decimal degrees, whereby the offshore Kirby and Oele (1975) and Morzadec-Kerfourn and Delibrias (1972) data points were rounded to 2 decimals to account for the greater positioning uncertainties. The latter data point is also described in Delibrias et al. (1974), but the reported coordinates plot onshore and hence are wrong. WGS-84 coordinates of the data point from Devoy (1979) were obtained from the UK sea-level database (Shennan et al., 2018).

3.2. Radiocarbon dating and calibration

All included samples are radiocarbon dates that were obtained over more than 50 years of research. The original reported dates from Jelgersma (1961; labelled as GrO-numbers) were later corrected for the Suess-effect by adding 240 ^{14}C yr (Vogel and Waterbolk, 1963) to the originally measured ^{14}C-age (Jelgersma, 1966) and relabelled to GrN-numbers. All other radiocarbon ages in the database are identical to the originally reported ones. In general, a "bulk error" of 100 ^{14}C yr is applied to bulk peat samples (cf. Hijma et al., 2015), but a 50 ^{14}C yr "bulk error" is applied to the bulk samples gathered by Van de Plassche and co-workers, because great care was taken in removing younger rootlets, and some smaller bulk samples that were dated using Accelerator Mass Spectrometry (AMS). Berendsen et al. (2007) revisited and redated sites of Van de Plassche (1982) to compare AMS-radiocarbon dating with earlier conventionally dated sample series, but they regard systematic differences in the mean age to be insignificant.

Except for the two samples of Kirby and Oele (1975), it is known that the reported ^{14}C-ages were corrected for isotopic fractionation. These two samples were derived from two lumps of undifferentiated peat on the seafloor. Kirby and Oele (1975) assumed the lumps to have been eroded from a transgressive peat bed that they found *in situ* in nearby cores. They describe that this peat bed covers Weichselian fluvial clay, a stratigraphic sequence very similar to the one near Rotterdam. We, therefore, expect the peat type to be predominantly fresh. For these two samples we applied an additional correction of -30 ± 20 ^{14}C yr, following Törnqvist et al. (2015), assuming δ^{13}C-values in the range of -28.5 to -25.5‰.

All radiocarbon dates have been (re)calibrated using OxCal 4.3 software (Bronk Ramsey, 2009) with the INTCAL13-curve (Reimer et al., 2013), rounding the result to the nearest 10 years. To assess which samples in the series of age-depth data points categorize as SLIPs and which are upper limiting points, 'unmodelled' individually calibrated age ranges were considered. In later steps of database preparation, the categorizing of the data points was used to obtain narrower age-ranges in a second calibration procedure. The density of data allows us to sort subseries of data points (i.e. grouped by site) on RSL age-depth position, exploiting the continuous RSLR trend seen in each subseries. In a next step, Bayesian models are applied that use that sorting to obtain 'modelled' calibrated age-ranges.

We formulated Bayesian radiocarbon calibration models in Chronological Query Language (CQL) built around the Sequence() function of OxCal (Bronk Ramsey, 2009). The Sequence() function operates ordinally (the user prescribes the chronological order of the dates), without any further consideration regarding depths of dated samples.

Four separate Sequence() models were run for the clusters of dates of the dune sites Hillegersberg, Barendrecht, Bolnes and Vlaardingen, one for the cluster of dates from the Maasvlakte site and one for the Southern Bight (scripts available in the data repository). The age models were constructed using only the basal-peat samples registered in the sea-level database, thus ignoring further local age constraints from additional dates on soils and strata immediately underneath the peats for example. At each site, we ordered the upper limiting data according to sample depth and inserted the SLIP dates into the sequence based on ^{14}C age and reconstructed RSL position (the latter is an outcome of procedures in sections 3.6-3.7). Nine out of 106 samples, all upper limiting data points from before 7.5 ka, were from sampling localities (e.g. Lower Scheldt and near offshore Southern Bight subsets) too isolated to slot them into any stratigraphic order and they were kept out of the Sequence() analysis. Legacy samples, notably those collected and conventionally radiocarbon dated 40 + years ago, have larger laboratory uncertainties than more recently collected ones, but the Bayesian calibration considerably narrows their age ranges. Also on the Rotterdam dune sites, where the accumulated data is a mix of legacy conventional dates and post-1990 more precise AMS dates, there are such effects. For the average sample, the Bayesian calibration reduced temporal uncertainty by 25%. Both the unmodelled and modelled ages are listed in the database.

For the interval defining the 8.45–8.2 ka sea-level jump event, a seventh Sequence() model was constructed. It is an expansion of that in Hijma and Cohen (2010), now allowing calibration of the onsets of two phases of accelerated sea-level rise in the RMD (Hijma and Cohen, 2010; Törnqvist and Hijma, 2012) using the SLIPs and dates bracketing the event. It includes additional event-dates from Rotterdam centre (Hijma and Cohen, 2010) and Maasvlakte (Vos et al., 2015), and the SLIPs and upper limiting dates from the database. Five combined dates below and five combined dates above the event were used to define the first onset age range (see discussion section). A series of SLIPs from after the first phase and two event-dates from the Maasvlakte area (Vos et al., 2015) bracket the second onset.

3.3. Stratigraphic position

The type of dated bed (mostly fen(-wood) peat, occasionally gyttja) is noted in the data-facies column. The database also

administers explicitly whether the top or the bottom of the bed was dated. The database further records sample overburden thickness and facies above and below the sample. This information was mostly available from the original sources and possibly feeds future (de)compaction offset and uncertainty quantifications. For offshore samples, we include the water-column height in the overburden thickness entries in the database.

3.4. Thickness and depth of sample in core or section

Information on thickness and depth of the samples was generally available from the original publications in proper detail, and only in a few cases it was necessary to estimate the thickness of a legacy sample. Often the samples with a non-reported thickness were part of a sampling campaign from which the thicknesses of other samples had been communicated, and in those cases, we substituted the missing thickness entries with a mean value. The sea-floor materials dated by Kirby and Oele (1975) were trawled peat lumps for which we estimated the thickness to be 0.1 m. Slupik et al. (2014) used a suction core that retrieved 0.5 m intervals of mixed sediments. They estimated the parent peat bed of their mixed sample to be 0.3 m thick.

We did not correct sample elevations for any post-depositional compaction of the underlying sediment, but did account for compaction of the sample itself by multiplying the thickness of the sample with a 'decompaction' factor. Van de Plassche et al. (2005, 2010) did so by using a minimum correction factor of 2.5 for the base of the dated sample and 3.5 for the top of the dated sample. Berendsen et al. (2007) used the same factors, although they erroneously reported factors of 1.5 and 2.5. Following Hijma et al. (2015) we simplified this approach by multiplying the thickness of the sample by a factor of 2.5 without changing the midpoint elevation of the sample. The sampling thickness uncertainty is half the 'decompacted' sample thickness. In this way, the increased uncertainty when using thicker samples is incorporated. This uncertainty is included in the corrected uncertainties (columns 72 and 73).

Vertical sampling uncertainties (sample-position accuracy) were set at 0.02 m, following Berendsen et al. (2007), when sampled from a core, a levelled section or a dredged peat block. Because Slupik et al. (2014) sampled from 0.5 m of mixed sediments, we set their sampling uncertainty at 0.25 m. From two building-pit outcrop samples (#5 and #10 from Hijma and Cohen, 2010) sample depths were determined using measuring tape and photographed scale-indicators, relative to a temporal benchmark of the constructor, and the sample-position accuracy of these samples was set at 0.1 m. Based on our familiarity with the hand-core and mechanical-core systems deployed in The Netherlands, we set the core shortening/stretching uncertainty at 0.05 m. For the mechanical-core systems, we assume the non-vertical drilling error to be zero due the usage of a spirit level. For hand coring we follow Törnqvist et al. (2004) and use −0.02 m per meter depth.

3.5. Elevation

In most cases, surface elevation was determined by levelling and tied to the national ordnance datum at the nearest benchmark. Note that the Netherlands' ordnance datum (known as Normaal Amsterdams Peil or NAP) over the period 1960-present was very similar to MSL along the Dutch shoreline (NAP = 0.114 m below Hook of Holland MSL in 2007; www.psmsl.org: RLR diagram Station 22). We put the levelling uncertainty at 0.01 m following Berendsen et al. (2007), and put the benchmark uncertainty at 0.02 m. The benchmarks are controlled every 10 years and its reference elevation updated and date stamped. In the first years after the control measurement, the accuracy is better than 0.01 m (Broekman and Kösters, 2010), but we set the uncertainty at 0.02 m to account for the decadal control interval. The surface elevation of one 21st-century data point was not levelled but extracted from a national coverage lidar dataset (AHN version 1) that has a 2σ-uncertainty of 0.35 m (Van der Zon, 2013).

The elevation of most offshore cores in the RMD were already corrected for the height of tide at the time of core collection. Following Hijma and Cohen (2010) we use an offshore depth uncertainty increase of 0.01 m/m. The water-depth uncertainty for the 1970's samples of Kirby and Oele (1975) and Morzadec-Kerfourn and Delibrias (1972) is set as high as 1 m because it is unknown whether a correction for the height of the tide was applied and which depth measurement system was used. The elevation of the sample from Devoy (1979) was originally tied to the U.K.'s O.D., with a measurement uncertainty of 0.1 m (Shennan et al., 2018). At the location of the sample, zero O.D. lies approximately 0.25 m below local MSL.

3.6. Tidal datums and palaeotidal changes

SLIPs are commonly defined with respect to a tidal datum, e.g. MSL or MHW. In most areas, the heights of these datums will have varied throughout the Holocene in response to sea-level change and related change in coastal configuration and water depth. In the absence of quantitative information of these changes, in many sea-level databases the modern heights of these datums as obtained from tide gauges near the sampling site are used and kept constant (see also Hijma et al., 2015). In our database, however, we make use of existing palaeotidal reconstructions for the Southern North Sea during the Holocene (Van der Molen and Van Dijck, 2000; Van der Molen and De Swart, 2001; Uehara et al., 2006). The palaeotidal simulations show that tidal influence in the Southern Bight began shortly after 10 ka BP. Tidal amplitudes gradually increased with deepening of the inundating North Sea and increased markedly when the southern and northern parts of the North Sea established a fuller connection (Fig. 4).

To use offshore palaeotidal reconstructions also for estimating elevations of paleotidal datums within the estuaries and back-barrier basins, it necessary to account for the altering of the incoming tidal wave. In all cases, a tidal wave will experience frictional dissipation after it enters the inlet and migrates through lagoons, basins and tidal channels. During the timespan covered by our data points, circumstances in the study area were such that the incoming tidal wave was further dampened by the flood-basin effect. This effect is basically caused by insufficient time during the flood and ebb phases to fill or drain the vast back-barrier area to the offshore MLW and MHW levels (Zonneveld, 1960; Van Veen et al., 2005). Starting with Van de Plassche (1980), several papers have discussed the role of the flood-basin effect in RSL-reconstruction context (Van de Plassche, 1982, 1995; Berendsen et al., 2007; Hijma and Cohen, 2010, 2011b; Van de Plassche et al., 2010; Vis et al., 2015). Building on this previous work, the palaeotidal fields in the database include an assessment of the flood-basin effect, uniformly re-evaluated for successive palaeogeographical developments in the lower RMD. An important aspect in this discussion is the role of palaeogeographical changes on the amount of tidal dampening through the flood-basin effect (Vis et al., 2015). The large amount of subsurface data in the RMD has allowed for mapping these changes to such an extent (Fig. 3; Hijma and Cohen, 2011a; Vos et al., 2011) that it is possible to make qualitative assessments of the degree of tidal dampening and to estimate the age of suspected change.

It is suggested that a full flood-basin effect was present in the Rotterdam between 6.5–3 ka BP (Van de Plassche et al., 2010),

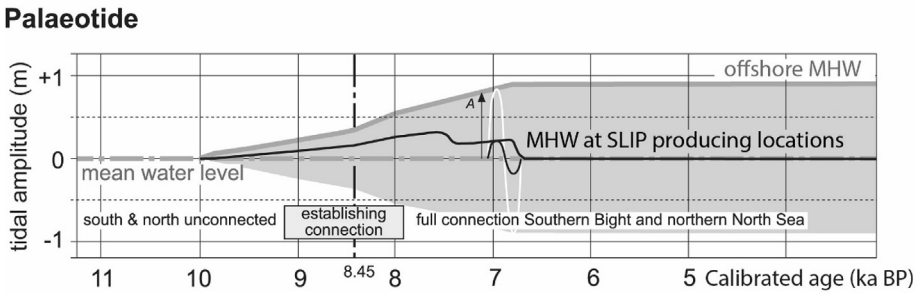

Fig. 4. The tidal amplitude offshore Rotterdam as it spun up while the Southern North Sea inundated (upper grey line), based on Van der Molen and De Swart (2001). The black line is indicative of the dampened tidal amplitude due to the flood-basin effect in the RMD SLIP providing area. The time line of the development of the connection between the Southern Bight and the northern North Sea subscribes to the following series of articles (Conradsen and Heier-Nielsen, 1995; Lambeck, 1995; Jiang et al., 1997; Van der Molen and Van Dijck, 2000; Uehara et al., 2006; Ward et al., 2016). Figure modified from Hijma and Cohen (2010).

meaning that inland MHW approached MSL and palaeogeographically this was the result of a vast expanse of back-barrier basins and lagoons in combination with lost numbers of tidal inlets. In this paper, we therefore use 100% dampening for the 6.5–3.0 ka BP samples. For older periods, we use 50% dampening for all pre-7.5 ka BP samples (cf. Hijma and Cohen, 2010), and 75% dampening for the 7.5–6.5 ka BP samples (Fig. 4). The increased flood-basin effect after 7.5 ka BP is an effect of the progressive infill of the Rhine-Meuse estuary near Rotterdam, under conditions of slowing RSLR and a proceeding avulsion of the Rhine main channel away from Rotterdam to a new northerly position (Hijma et al., 2009; Hijma and Cohen, 2011a). This resulted in a reduced tidal inlet width and decreased mean water depth in the estuary inshore (tidal channels remained deep, but shoals shallowed and grew in area) and a more pronounced flood-basin effect in the Rotterdam area, in line with Van de Plassche et al. (2010). An estimate of the total uncertainty involved with the above procedure is calculated by taking a percentage of the used offshore paleotidal amplitude for each data point, hereby accounting for larger uncertainties for older time periods (pre-7.5 ka BP: 37.5%; 7.5–6.5 ka BP: 25%; post-6.5 ka BP: 18.25%). The relative uncertainty of the dampening factor increases back in time, because the tidal configuration of the North Sea was more uncertain.

Since palaeotidal models indicate that the present-day tidal amplitude (0.9 m) was reached around 6.8 ka BP, we use that amplitude for samples younger than 6.8 ka BP. For samples older than 6.8 ka BP, we use palaeotidal modelling results from Van der Molen and De Swart (2001; hereby calibrating their radiocarbon age time stamps to calendar years), which were later corroborated by Uehara et al. (2006). This means that between 10 and 8.5 ka BP we incorporate a linear spin up of tidal amplitude offshore Rotterdam from 0 to 0.35 m (see also Fig. 4), and from 8.5 to 6.8 ka BP a linear increase from 0.35 to 0.9 m (corresponding to the modern value). Using these linear functions and the mean age of each SLIP, we calculated the contemporary offshore MHW for each SLIP and rounded off to 1 decimal. For the data points of Kirby and Oele (1975), Morzadec-Kerfourn and Delibrias (1972) and Devoy (1979), that lie outside the study area of Van der Molen and De Swart (2001), we used palaeotidal output from Uehara et al. (2006).

The above is incorporated in the database as follows. The MHW-column in the database (column 47) contains the present-day MHW value near the sampling site and from this the reference water level (RWL; see also next section) is calculated (column 57). The palaeo-RWL value is listed in column 61 and calculated by applying a flood-basin effect factor to the modelled palaeotidal MHW-value. Because applying an offshore-to-inshore tidal dampening calculation is not standard protocol in the database format chosen for this special issue (it does not have dedicated new database fields for it), the RMD database lists the flood-basin effect factor and the palaeo-MHW values as notes with each data point (column 77).

3.7. Indicative meaning: separating SLIPs from upper limiting data points

Almost all data points in the database are freshwater peats of various clay-content and botanic compositions (Bos et al., 2012). All dated peat beds are considered to have formed at a vertical position that reflected contemporary local GWLs. The organic beds are regarded to have formed through accumulation of plant material around GWL, allowing for semi-daily rewetting and hence waterlogged preservation of the organics that settled below GWL. This process was further helped by the steadily rising trend of GWL (Cohen, 2005). In the database we have specified peat-type dependent water-depth offsets (upwards) and specified indicative-range uncertainties, as listed in Table 1. For the peats that cover the flanks of inland dunes, the relationship between the elevation at which the indicators formed and contemporary sea level was intensely studied and discussed in The Netherlands (see Van de Plassche and Roep, 1989 for an overview of this discussion). In choosing a RWL, workers opted to relate the dune flank basal-peat samples from the Rotterdam area to either MSL or to MHW, until Roep and Beets (1988) used palaeotidal markers in coastal barrier and other littoral deposits to construct sea-level curves that, although independently derived, matched well with the sea-level curves based on freshwater peat beds. This confirmed the interpretation of Van de Plassche (1982) that in the back-barrier 'intracoastal' areas fed by the RMD, the water levels in which the peats formed were maintained around local MHW levels (dampened relative to inlet and offshore tides, as discussed above).

In this paper, we also tied the formation of age-depth points in each time frame to MHW tide-datum levels, but used different RWLs and indicative ranges for the different types of peat and settings to compensate for the water depth in which the peat or organic layer formed (Table 1). First, samples taken from the top of basal-peat beds that are directly overlain by brackish, tidal deposits were categorized as SLIPs directly. Next, the samples taken from the bottom of basal-peat beds were plotted in ensemble. When data from a relatively small area are plotted they show a sigmoidal groundwater-level curve with a slowly rising pre-transgression limb (upper limiting data points) that ends at an inflection point, after which the curve is fully controlled by sea level and rises at the same pace as contemporary RSL (see also Hijma and Cohen, 2010). The bulk of the age-depth data from after 8.0 ka (inland dune sites) groups closely together along the RSL-trend. From them the youngest-deepest were categorized as SLIPs and the slightly older

Table 1
Summary of the indicative meanings of the different sample types in the Rhine-Meuse Delta sea-level database. SLIPs come from either tops of basal-peat beds that are directly overlain by tidal deposits or from bottoms of basal-peat beds if they plot on the *youngest-deepest* side of the dataset (see main text for additional explanation).

Sample Type	Evidence	When selected as SLIP (Sea-Level Index Points)		Otherwise (Upper Limiting Data Points)	
		Reference Water Level	Indicative Range	Reference Water Level	Indicative Range
Fen-wood peat	Generally formed in an *Alnus-Salix* swamp (Bos et al., 2012). Observations of modern analogues indicate this type of peat formed very close to average water levels (Clerkx et al., 1994). The indicative range of ±0.1 m follows Törnqvist et al. (1998).	MHW	MHW ±0.1 m	GWL	GWL ±0.1 m
Fen peat on aeolian-dune flanks	Generally consisting of *Phragmites* or *Phragmites-Carex* peat, plant types that can form in water depths of more than 0.5 m (Den Held et al., 1992). On dune flanks, however, significant water depths can be excluded. Water depth (0.1 m) and indicative range (±0.2 m) follow Berendsen et al. (2007).	MHW-0.1 m	(MHW-0.1) ± 0.2 m	GWL-0.1 m	(GWL-0.1) ± 0.2 m
Fen peat	For fen peat that did not form on a dune flank, average water depth is set at 0.3 m and indicative range at ± 0.2 m, following Hijma and Cohen (2010).	MHW-0.3 m	(MHW-0.3) ± 0.2 m	GWL-0.3 m	(GWL-0.3) ± 0.2 m
Undifferentiated peat types	For peat beds of unspecified botanical composition, we use an average water depth of 0.2 m with an indicative range of ±0.3 m to cover the full range of water depths in which fen-wood or fen peat generally forms.	MHW-0.2 m	(MHW-0.2) ± 0.3 m	GWL-0.2 m	(GWL-0.2) ± 0.3 m
Gyttja organic beds	Gyttja deposits are relative poor water-level indicators, since they can form in significant water depths. Following Hijma and Cohen (2010) we assume an average water depth of 0.75 m and an indicative range of ±0.5 m.	MHW-0.75 m	(MHW-0.75) ± 0.5 m	GWL-0.75 m	(GWL-0.75) ± 0.5 m

or higher data points as upper limiting data points. The relatively high position of the non-SLIP data points can either be the result of less tidal dampening than assumed (for the most seaward points) or be the influence of the RMD river gradient for the more landward points.

The river-gradient effect (Louwe Kooijmans, 1974) describes the phenomenon that local groundwater, and hence tidal, levels tend to get raised by the river gradient in an upstream direction, in similar amounts as channel-belt gradient lines of contemporary rivers. In addition to the regional longitudinal slopes in the delta plain, river-gradient effects can be considered to have varied locally owing to branch avulsions, which make new distributaries develop and older ones abandon. In the last 7.5 kyr, such avulsions happened mainly upstream of the study area (Stouthamer and Berendsen, 2000), where they have lead to substantial GWL-height changes in affected flood basins (Van Asselen et al., 2017). Avulsive abandonment of a branch generally leads to a lowered flood basin GWL (dropped river gradient), while initiation ofa new branch can raise flood basin GWL (increased river gradient). Such effects have also presumably affected the flood basins hosting the inland dune sites in our study area (Berendsen et al., 2007; Van de Plassche et al., 2010), where this must have interacted with local tidal range (Van Asselen et al., 2017).

For dates that categorize as SLIPs, additional processing was executed, the outcomes of which were stored in separate database fields. This step-wise converted the MHW-related SLIPs to MSL-related ones, whereby additional vertical offsets are applied (downward, see below) and vertical uncertainties finalized. To be consistent with the procedure for the SLIPs, we also apply a correction for water depth at time of formation and calculate the vertical uncertainty around the established GWL to the upper limiting data points. For these points the GWL is used as the reference water level.

3.8. Relative sea-level and uncertainty

For samples categorized as SLIPs, RSLs were calculated by subtracting the RWL from the elevation of the dated sample (column 68). For upper limiting data points, this column stores GWLs. In column 71 we correct the RSL values for the modelled palaeotidal changes (0.13 m on average) and use the corrected RSL values in subsequent analyses and figures. The approximate 2σ-sigma vertical uncertainty is calculated by taking the square root of the quadratic sum of all individual sources of uncertainty, with columns 72 and 73 including the palaeotidal and decompaction uncertainties.

For the calculation of rates and sea-level trends (see Figs. in next section) we used the EIV-IGP model of Cahill et al. (2015, 2016). EIV stands for 'Errors-In-Variables' and is used to take the uncertainty in age into account. IPG stands for 'Integrated Gaussian Process' and this approach is used to estimate the non-linear trend underlying the noisy sea-level data.

4. Results

The 50 SLIPs and 56 upper limiting data points in the Rhine-Meuse delta RSLR database are plotted in Fig. 5 as a data overview figure. The SLIPs cover an age-range of 8.8–3.0 ka BP and are available from the Rotterdam and Maasvlakte areas, but not for further offshore. For upper limiting data points, the coverage does extend offshore, reaching back to 11.5 ka BP in the Rhine-Thames confluence zone.

The step of Bayesian radiocarbon calibration (from unmodelled to modelled 2σ on the time axis) affected 'younger' SLIPs from the Rotterdam area modestly (most notably at 8.4–8.0 and at 6.5–6.0 ka BP) and affected older SLIPs of the Maasvlakte area (9.0–8.0 ka BP) most markedly. At first sight, the difference in result may be counterintuitive because the uncertainty is larger for the Rotterdam area and hence for the younger SLIPs. In part, this may be a graphic artefact because of overlapping post-8 ka BP SLIPs, but the difference in uncertainty may also have geological origins resulting from the following:

1. Before and after 8.0 ka, vertical uncertainty (±0.2–0.3 m at 2σ) and unmodeled 2σ dating uncertainty (AMS-dated ±180 cal yr; conventional: ±240 cal. Yr) for typical data points have similar values. The difference is in the rate of RSL change which after 8.0 ka was decelerating due to decreasing rates of eustatic SLR, and in the study area drops markedly from >10 mm/yr before 8 ka to 3 mm/yr around 7 ka.
2. For the post 8-ka part of the data series, the deceleration results in temporal overlap of data points. The gain from Bayesian calibration – also owing to our conservative choice of not introducing any further boundaries within the Sequence()-scripts for the four Rotterdam river dune sites – in the post-8 ka part of the data set is mainly that of narrowed uncertainty

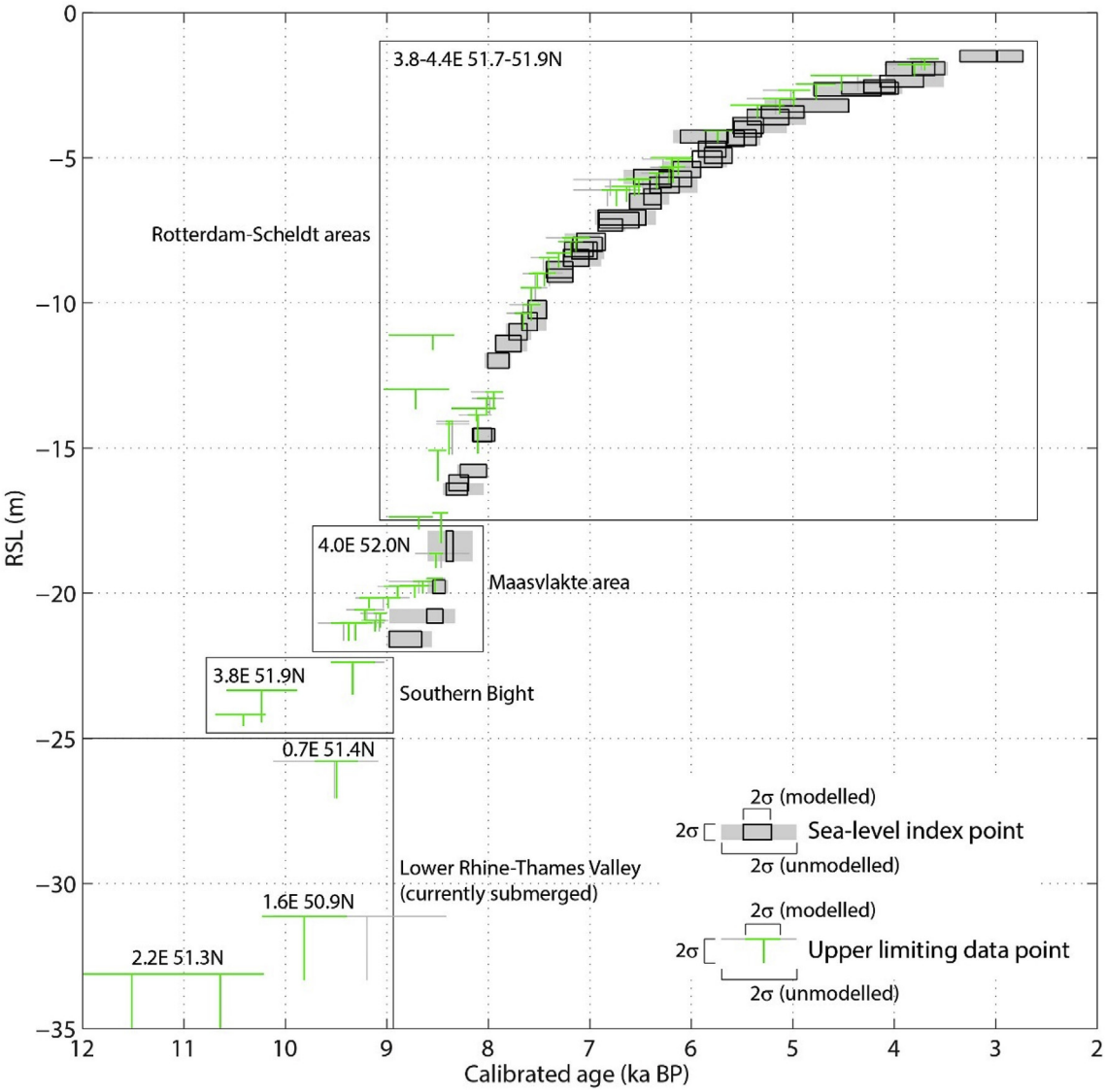

Fig. 5. Plot of all SLIPs and upper limiting data points in the database for the different areas (see Figs. 1 and 2 for locations) with their approximate lat/long coordinates. Because the Strait of Dover and RMD have distinctly different GIA histories and tectonic settings, the figure as a whole does not reflect rates of RSLR for a fixed location, but rather where and when peat formation started to form in the moving river-mouth areas.

of conventionally dated samples at positions in the sequences between AMS samples of greater dating precision, but the resultant modelled age-range series is still one with overlap (less so if individual dune sites are plotted separately).

3. For the pre-8-ka part of the data series, the rapid rise results in clear vertical separation of peat beds, formed within a short time and intercalated with gyttjaic organo-clastic muds. In that sedimentary setting, the CQL-scripted Bayesian modelling is not conservative, and Boundary-statements were included in the Sequence-scripts (see section 3.2). This forces the modelling to produce age-range series that within subsets maintain considerable overlap, but at said boundaries enforce step shifts. This results in a higher gain of Bayesian calibration for the 9–8 ka data points (40% reduction of 2σ age range), then for the post 8-ka data points.

Fig. 6, which zooms in on the SLIP-covered time period (9.0–3.0 ka), shows the database entries together with the most-recently published hand-drawn RSLR reconstructions for the Rotterdam area (see section 5 for a discussion of these curves). We have further plotted 1-σ and 2-σ confidence intervals of the EIV-IGP model of Cahill et al. (2015, 2016) using the modelled calibrated ages. The EIV-IGP modelling generally reproduces the constructed curves, with a particularly tight uncertainty band before 8 ka BP, when modelled rates of RSLR were very high (over 10 mm/yr). Between 8 and 7 ka, rates quickly drop from 9 to 3 mm/yr and after 7 ka deceleration decays towards a ~1 mm/yr background rate at ~4.5 ka BP. Between 8.45–8.2 ka BP the RSL curve of this paper has marked acceleration and deceleration events that are not reproduced by the EIV-IGP model (Fig. 6). This part of the curve incorporated additional sedimentological and event-stratigraphical information in the Bayesian radiocarbon calibration, that could not be fully considered in the EIV-IGP modelling. In other words, the EIV-IPG model should be regarded to reproduce a smoothed signal of the pre-8.2 ka sea-level jump event. This event, and possible other fluctuations, are discussed in the next sections, preceded by a comparison of the results from this database with hand-drawn sea-level reconstructions for the RMD.

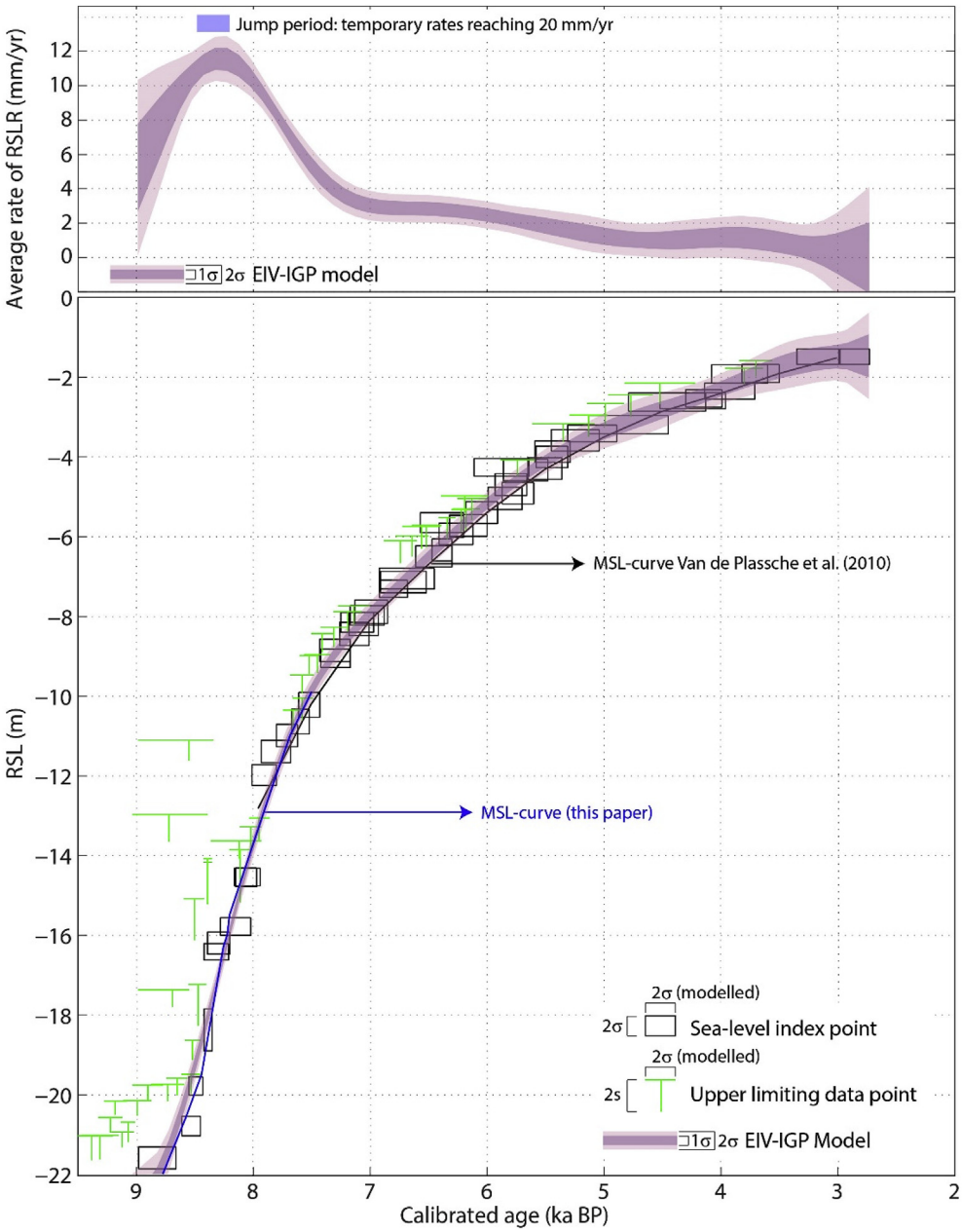

Fig. 6. Plot of the SLIPs and the upper limiting data points for the wider Rotterdam area (see Fig. 2), including the MSL-curve of Van de Plassche et al. (2010) and the revised MSL-curve of Hijma and Cohen (2010) for the 9–7.5 ka BP period (this paper) that is further discussed in section 5.1. The timing and magnitude of the sea-level jump is discussed in section 5.2. The confidence intervals and the rates were calculated with the model described in Cahill et al. (2015, 2016). During the sea-level jump period, average rates of RSLR reached ~20 mm/yr based on the duration and magnitude of the jump. This rate includes a RSLR-background rate of 10 mm/yr (see section 5.2.2).

5. Discussion

5.1. Comparison with existing sea-level reconstructions for the Rhine-Meuse delta

Fig. 6 shows the MSL-reconstructions of Van de Plassche et al. (2010) and Hijma and Cohen (this paper) together with the SLIPs and upper limiting data points. The reconstructions are based on different types of basal peat (aeolian-dune flank peat versus mostly palaeovalley-floor peat), have some overlap in the 8.0–7.5 ka BP time window and were constructed in different manners.

Van de Plassche et al. (2010) related and plotted their SLIPs to back-barrier MHW and drew a MSL-curve below selections of these points, hereby accounting for changes in the flood-basin and river-gradient effects. Using the protocol presented in this paper, the data from Van de Plassche et al. (2010) are now related and plotted directly to MSL. Fig. 6 shows that in all cases their reconstructed MSL-curve crosses the boxes of the SLIPs. This is encouraging in terms of cross-validation and mutual validity of our database approach and original findings regarding variable tidal dampening and river gradient. The advantage of the database approach is that it provides a more objective, transparent and reproducible way of deriving a sea-level curve from source data (besides making it readily available in a database format). Since in the database a 50 or 100 ^{14}C yr error is assigned to bulk samples, the horizontal 2σ-range of the boxes in Fig. 6 is larger than those used in Van de

Plassche et al. (2010). The curve mostly falls within the calculated 68% and 95% confidence intervals. The largest deviation occurs between 7500 and 6000 BP where the curve of Van de Plassche et al. (2010) plots lower.

The MSL-curve from the current paper is a revision of the one in Hijma and Cohen (2010), a curve that was based on a database protocol that differs in small details from the one used here. The differences are mostly caused by added uncertainties associated with the coring-process, some changes in palaeo-MHW values and in the indicative meaning. If the plotting of SLIP boxes in the original and the current paper are directly compared, one will find the average centre points to have shifted a few decimeters downward and the uncertainties to have changed mostly a few centimeters. Because of these differences, the MSL-curve plotted in Fig. 6 is not identical to the curve of Hijma and Cohen (2010). The revised curve also uses 18 new data points that have become available for the 9–8 ka BP period since 2010 (4 SLIPs and 14 upper limiting data points). Together with information from recent papers from other regions describing the pre-8.2 ka sea-level jump, the new SLIPs have also been used to detail RSLR around this jump.

5.2. The structure of the pre-8.2 ka sea-level jump in the RMD

As first concluded in Hijma and Cohen (2010), the RMD SLIPs over the period 9.0 to 8.0 ka BP show that a marked sea-level jump preluded the 8.2 ka cooling event, an event that resulted from the impact of the drainage of Lake Agassiz-Ojibway and the associated melt-water pulse (Barber et al., 1999; Törnqvist and Hijma, 2012). The next section reiterates the argument for the identification of a RMD sea-level jump in this period and links this jump to the global record. It is followed by an update of the age-control and magnitude of the jump using the new sea-level data for the RMD.

5.2.1. Earlier work and correlation of the RMD record to the global record

By dating a regional flooding surface multiple times and at several locations in the RMD, the onset of the sea-level jump was directly dated by Hijma and Cohen (2010) to 8.45 ± 0.44 ka BP. This timing was derived by bracketing an event contact in the same study area, independently from GWL/MHW analysis and SLIP identifications. The main arguments for labelling the RMD event a sea-level jump, instead of e.g. a local transgressional event, are that the flooding surface can be traced across a large area (778 km^2) and consists of an abrupt gyttja-over-peat contact. Such a laterally extensive contact is highly indicative of a sudden change in relative sea level (cf. Nelson et al., 1996; for an area with frequent co-seismic subsidence). In the basin setting of the RMD, a co-seismic event would imply a sudden downward movement of the basin shoulder (Maasvlakte area) relative to areas nearer to the depocentre (Rotterdam area), which is at odds with the normal fault direction. From a sedimentary perspective, the most plausible cause for the sudden change is therefore a sea-level jump. The inference is further strengthened by event contacts of similar age in deltas around of world, and a region where a meltwater pulse was sourced.

Quantification of the jump magnitude in the RMD relies on SLIP identification for periods before and after the event in the Maasvlakte and Rotterdam areas respectively. In the Hijma and Cohen (2010) paper a total magnitude of 2.11 ± 0.89 m was derived for the sea-level jump, on top of background RSLR. Because finger-print modelling for Laurentide-released melt-water pulses indicates the RMD should have experienced about 70% of the globally averaged jump (Kendall et al., 2008), the magnitude at far-field locations corresponds to 3.0 ± 1.2 m. This was presented as the total magnitude of a presumably two-phased jump event stretching the time period 8.45 to 8.25 ka BP (see also Törnqvist and Hijma, 2012).

The sea-level jump was also studied in the near-field Mississippi River Delta (Li et al., 2012), the far-field Yangtze delta (Wang et al., 2013); in the Rhone (France; Amorosi et al., 2013) and Po deltas (Italy) and at rebound sites in Scotland (Lawrence et al., 2016), with differences with respect to timing and total magnitude. The work in the Po Delta has identified the event as a clear transgression surface that can be mapped in the lower Po Delta over distances of 20 km. Similar to the RMD, the transgression is recorded and dated using swamp basal peats that are conformably overlain by subaqueous muds (8.5–8.2 ka BP; Amorosi et al., 2017; Bruno et al., 2017).

From multiple lines of evidence, i.e. glaciogenic sedimentary observations in former lakes Agassiz and Ojibway (Lajeunesse and St-Onge, 2008; Roy et al., 2011; Daubois et al., 2015), glaciomarine observations in the Hudson Bay, Tyrrell and Labarador seas (Ellison et al., 2006; Lewis et al., 2012) and cave data (Domínguez-Villar et al., 2009), it is clear that the pre-8.2 ka sea-level jump has a complex structure (Carlson and Clark, 2012), that may be further constrained by including detailed RSL studies from different parts of the world (Törnqvist and Hijma, 2012). In 2010, the RMD observational data was insufficient to independently reveal the internal structure of the sea-level jump. Since then, the indications that the drainage of Lake Agassiz occurred in at least two phases have become more clear in the global literature as well as in the data from the RMD.

From a series of sites in Scotland, Lawrence et al. (2016) describe three phases of increased rates of RSLR, starting at 8.76–8.64, 8.60–8.47 and 8.32–8.22 ka BP, respectively. They link the latter two phases to Lake Agassiz-drainage events and the first to the opening of the Tyrrell Sea and associated increased melt of the Laurentide ice sheet (LIS). These timings and correlations match those from the RMD, although in the RMD a slightly younger onset of the first Lake Agassiz event is derived. Considering that the Scotland age-brackets result from interpolating between radiocarbon dates, this difference can be resolved. The RMD timing is based on direct dating of a sedimentary event and is hence regarded more precise than an interpolated age between SLIPs. The start of the last drainage event as recorded in Scotland is in close agreement with that of the onset of acceleration in the Mississippi Delta, which is dated to 8.31–8.18 ka BP (Törnqvist et al., 2004; Li et al., 2012). In the Yangtze delta, around 6 m of RSLR is observed between 8.6 and 8.3 ka BP and 3 m between 8.3–8.0 ka BP. Because the 8.3–8.0 ka BP period largely postdates the sea-level jump, this indicates a Yangtze-delta background rate of RSLR of ~1 m/century to apply. For the 8.6–8.0 ka BP period, this suggests RSLR to have included a sea-level jump of ~3 m. The timing (8.6–8.3 vs. 8.5–8.2) and far-field totalled magnitude of the jump (~3 m) match the independent magnitude estimates of the RMD (Hijma and Cohen, 2010; this paper) and jump-event internal phasing results from Scotland (Lawrence et al., 2016) and the Ojibway-Hudson Bay-Labrador Sea source region (references above).

5.2.2. Updated age-control and magnitude of the pre-8.2 sea-level jump event

Since 2010 new RMD sea-level data have been gathered in the time-interval of interest, and they begin to reveal the RSL impact of the Lake Agassiz-Ojibway drainage-event phases (Fig. 7) and also enable updated calculations from Hijma and Cohen (2010). In that paper we used combined dates from below (peat, n = 5) and above (gyttja, n = 3) the event contact to calculate the *terminus post quem* (here TPQ1) and *terminus ante quem* (here TAQ1) for the event. In the current paper, we repeated this routine, but now using the latest IntCal13 calibration-curve (Reimer et al., 2013), with more conservative dating uncertainties for bulk samples (section 3.2) and using the in-sequence calibrated ages (see section 3.2).

The TPQ1 dataset has been unchanged from Hijma and Cohen

(2010), but to the TAQ1 dataset we added two dates from the gyttja layer above the peat. One is a SLIP in the database (ID = 50; POZ-36943), while the other has not been included in the database, because for this sample it is not clear whether the sediments above the gyttja layer were deposited in a brackish and tidally-influenced environment. Still, we regard this peat-gyttja transition as part of the event contact (GrA-55011, described in Vos and Cohen, 2014; Vos et al., 2015). These bracketing dates indicate that the jump started at 8.44 ± 0.41 ka BP (1σ), nearly identical to the calculated onset in Hijma and Cohen (2010). This age is used for the knickpoint in Fig. 6 that marks the onset of the sea-level jump and is thus now based on 10 radiocarbon dates that bracket the event contact.

Hijma and Cohen (2010) used the first SLIP after the start of the sea-level jump to calculate the total magnitude of the jump. During the jump the zone of peat formation shifted 30 km landward and the dated peat layer was interpreted to have formed during a phase of renewed peat formation that could only start after the rate of RSLR decreased to it background value of ~10 mm/yr (such critical rates of RSLR for RMD transgressive basal-peat formation are also derived by Cohen, 2005; Peeters et al., 2018). The current database now holds more SLIPs that formed after the sea-level jump, hereby giving more body to the interpretation of renewed peat formation at the end of the first phase of accelerated RSLR.

The lowest new SLIP (in the Maasvlakte area; gyttja) pulls the lowest part of the reconstruction of Hijma and Cohen (2010) to the younger side. The next in line (Korendijk, Wassenaar; peat) comes from the flanks of the palaeovalley (Fig. 2) and also plot to the younger side of the earlier reconstruction. If the reconstruction of Hijma and Cohen (2010) is accepted, this would imply that groundwater tables stood significantly lower along the flanks of the valley compared to the centre of the valley, which is unrealistic (see also Koster et al., 2017). We therefore revised the RMD SLR-curve between 8.4 and 8.0 ka BP (Fig. 7), also in the light of the envisaged two-phased structure of the sea-level jump. The revised curve has a first acceleration beginning at 8.44 ± 0.41 ka BP (see above) and a second one starting tentatively at 8.22 ± 0.65 BP (1σ). This latter age is based on the definitive, widespread and well-dated drowning of the Maasvlakte area (Vos and Cohen, 2014; Vos et al., 2015; combined age of POZ-36942 and POZ-36915); hereby confirming the ages of Yu et al. (2012) and Lawrence et al. (2016) for what we consider the second phase.

In a next step of reassessing the pre-8.2 jump, the improved chronological constraints have been used to redo and refine jump-magnitude calculations. For this we use a background rate of

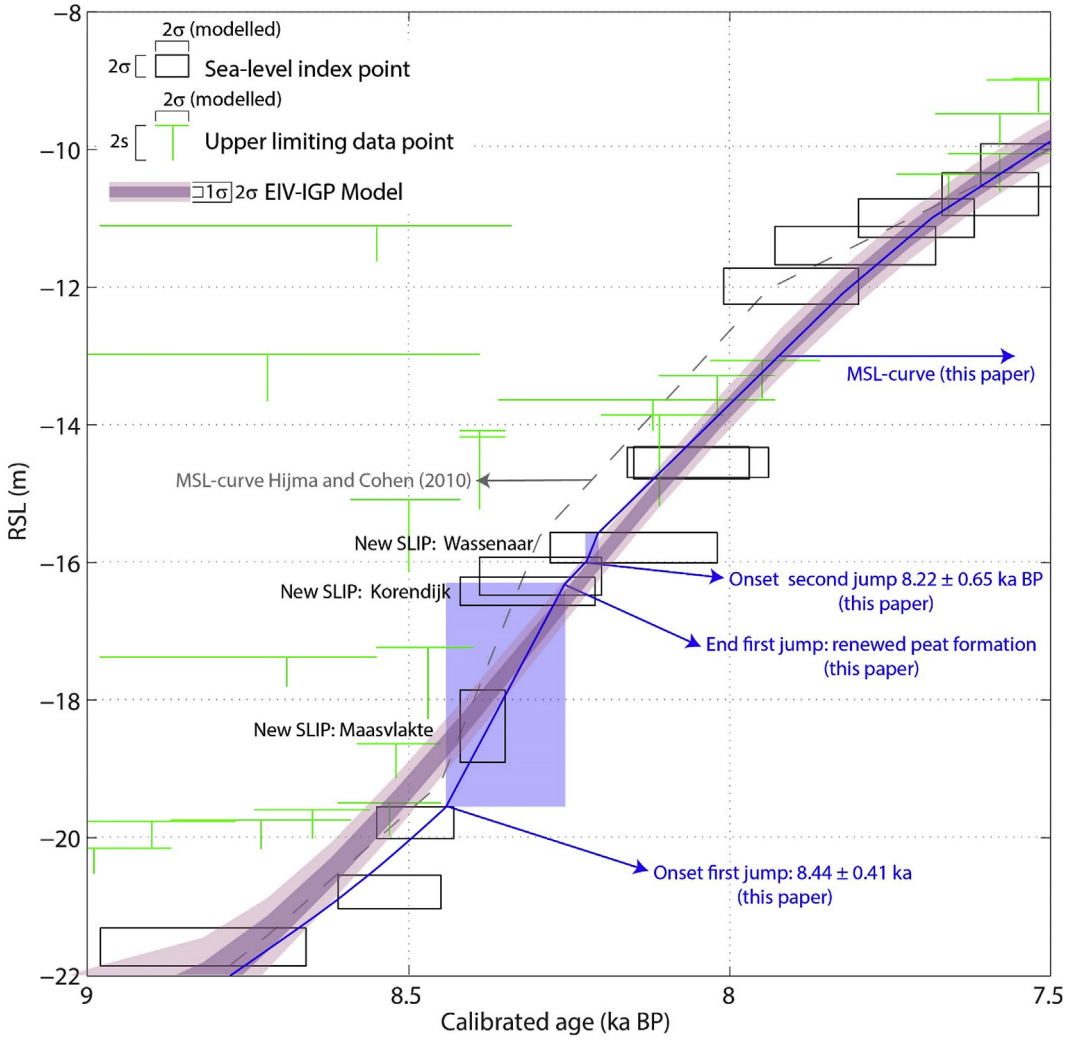

Fig. 7. Plot of the SLIPs and the upper limiting data for the period 9–7.5 ka. The confidence intervals were calculated using the model described in Cahill et al. (2015, 2016). The two purple boxes represent the periods in which the two sea-level jumps occurred. (For interpretation of the references to colour in this figure legend, the reader is referred to the Web version of this article.)

10 mm/yr RSLR (unchanged from Hijma and Cohen, 2010) just before, between and directly after the jump phases. The trade-off in magnitude of the first versus the second phase is based on the 2 SLIPs just below −16 m RSL that we consider to have formed in between the phases of accelerated SLR. This would mean that the first phase of the sea-level jump in the RMD was 1.7 ± 0.6 m (1σ, see sheet Jump-Magnitude Calculation in the data repository) and significantly larger than the second phase, in line with the relative magnitudes in Lawrence et al. (2016). The second phase of the jump can only have been a few decimeters max (estimated at 0.2 ± 0.2), because we regard the SLIP from Wassenaar (Fig. 7) to have formed after the onset of the second phase and the two preceding SLIPs before this onset. The combined local magnitude would thus be close to 2 m, hereby confirming the earlier work of Hijma and Cohen (2010). The two phases correspond to globally-averaged jumps of 2.5 m ± 0.9 m (1σ) for the first and 0.3 ± 0.3 m (1σ) for the second phase (based on a recorded 70% in the RMD; Kendall et al., 2008).

While we consider the calculated onsets to be robust, the timing of the end of the two phases of accelerated RSLR is tentative. Note that this uncertainty does not influence the magnitude calculations. The reconstruction in Fig. 7, with its linear segments, should therefore be seen as the subjective average of a suite of possible event-resolving sea-level reconstructions, and the communicated uncertainty ranges encompass these. When we compare the linear-segmented jump reconstruction with the results of the EIV-IGP model there is significant deviation around the time of the jump. This is mostly due to the fact that the model was only fed with SLIPs, while we also used additional event-bracketing data and sedimentological information that, at this point, cannot be used in the model. If a future version of the model could use such information, this would have great added value. In addition, the model uses a covariance function that imposes smoothness, in this case meaning that the offset position of some SLIPs around the jump can potentially be regarded as noise by the model.

5.3. Younger acceleration events, such as around 7.6 ka BP?

Several papers mention an acceleration in the rate of RSLR around 7.6–7.4 ka BP, with Yu et al. (2007) proposing a semi-instantaneous jump of 4.5 m at 7.6 ± 0.2 ka BP along the Swedish Baltic Coast, and Blanchon et al. (2002) and Bird et al. (2007) also suggesting a meter-scale sea-level jump beginning around that period. The source for this jump is sought in increased LIS retreat (Carlson et al., 2008). Recent work from the Po Delta indicates a marked transgressive phase starting ~7.7 ka BP (Amorosi et al., 2017; Bruno et al., 2017). If we zoom in at the RMD-curve for that period (Fig. 8) we see that the confidence intervals show a steadily decreasing rate of RSLR, leaving no room for meter-scale sea-level jumps. There is an absence of SLIPs around 7.4 ka BP, which could either be a sign of increased rates of RSLR or of just a relatively less sampled time-frame. The potential increase in rate is relatively small though and can only be further studied after additional detailed sedimentological investigations.

For the time window 7.5 to 3.0 ka BP (Fig. 6), the presence or absence of acceleration and deceleration events in the RMD curve have been a point of discussion in the classic works of Jelgersma (1961) and Van de Plassche (1982) and reiterated since. With the growth of the number of data points, the RMD sea-level curve has become increasingly smoothed. Also after categorization of screened selections of data points as either SLIPs or upper limiting points (Van de Plassche, 1995; Van de Plassche et al., 2010; this paper), a SLR curve of smooth nature is retained for the youngest 7.5 ka, although periods of relatively small accelerations have been suggested (see e.g. Denys and Baeteman, 1995). The overall trend between 8.0 and 3.0 ka BP shows gradually decreasing rates of RSLR due to decreasing post-glacial eustatic inputs and residual glaciohydro-isostasy components (Kiden et al., 2002; Vink et al., 2007; Lambeck et al., 2014; Peltier et al., 2015).

5.4. Connecting a Southern Bight palaeovalley SLR curve to the RMD

In line with our efforts to get maximum SLIP yields out of larger datasets of basal-peat index points from valley sections in the onshore (Rotterdam) and near-coastal areas (Maasvlakte), we here complete our discussion of such data for the remainder of the Rhine-Meuse palaeovalley and its larger tributaries (Scheldt, Thames, Medway) further offshore in the Southern Bight (Fig. 1). The reasons to do this are (1) to demonstrate the screening method for upper limiting vs. SLIP data points in a data poor environment; (2) to be complete when describing the record of 'Rhine-Meuse valley transgression' in our cross-comparisons with other deltaic systems (notably the Po and Yangtze Deltas); (3) to provide target curves to steer renewed data collection through cruises offshore. For the Southern Bight, the discussion below should help cruises with RSLR and GIA quantification goals, as well as provide improved first-order time control and taphonomic understanding of the Holocene capped sea floor to offshore archaeological and palaeoenvironmental studies.

Rather than approaching offshore legacy data with a pessimistic view, such as not meeting modern standards of accuracy, introducing scatter, and extending age-depth plots to larger than preferred study areas (that would introduce false trends and/or scatter because of GIA and tectonic subsidence differences), we instead outline constructive approaches to connecting reconstructions from the land to the offshore. By restricting our offshore data selection to the course of the palaeovalley only, scatter is reduced. For the time period before 8.8 ka BP, the database contains upper limiting data points only. In a set of upper limiting data points, a modest amount of scatter is natural, as comparison with the younger part of the data set illustrates.

Below we will discuss our RMD-offshore data points in two groups: (1) the set from above −25 m O.D. collected in the vicinity of the Dutch coast (box Southern Bight in Fig. 5), marking swamp formation between c. 9.5 and 8.5 ka BP, in the reach of the Rhine-Meuse palaeovalley where it was joined by the river Scheldt (Figs. 2 and 3); and (2) the set collected at greater depths further downstream (box Lower Rhine-Thames Valley in Fig. 5), from older transgressed swamp-environments in the reach where the Rhine-Meuse-Scheldt palaeovalley was joined by the rivers Thames, Medway from the UK side, and IJzer from the Belgian side (Bridgland and D'Olier, 1995; Hijma et al., 2012). In using the palaeovalley path to constrain our selection of offshore data points, we set up the offshore data in a way that allows us to use similar screening techniques as applied to coastal-delta plain buried environments (this paper). This valley-longitudinal way of plotting differs from along-coast data-overview approaches common in GIA exploring studies (Shennan et al., 2000; Vink et al., 2007) and from all-inclusive approaches in offshore data presentation (e.g. Jelgersma, 1979). Keeping the selection to the Rhine-Meuse trunk valley and lower reaches of immediate tributaries is also the reason that data points further north in the Southern Bight (Jelgersma, 1979; Kiden et al., 2002) are not included in our age-depth plots. RSL curves drawn based on a valley-longitudinal age-depth plots are representative of the river mouth, which shifts landwards with the rising sea. It should be realized that the Strait of Dover and RMD areas have distinctly different GIA histories (Vink et al., 2007) and tectonic settings, and paleovalley-longitudinal combination plots such as Fig. 5 should not be used to infer rates of RLSR for fixed

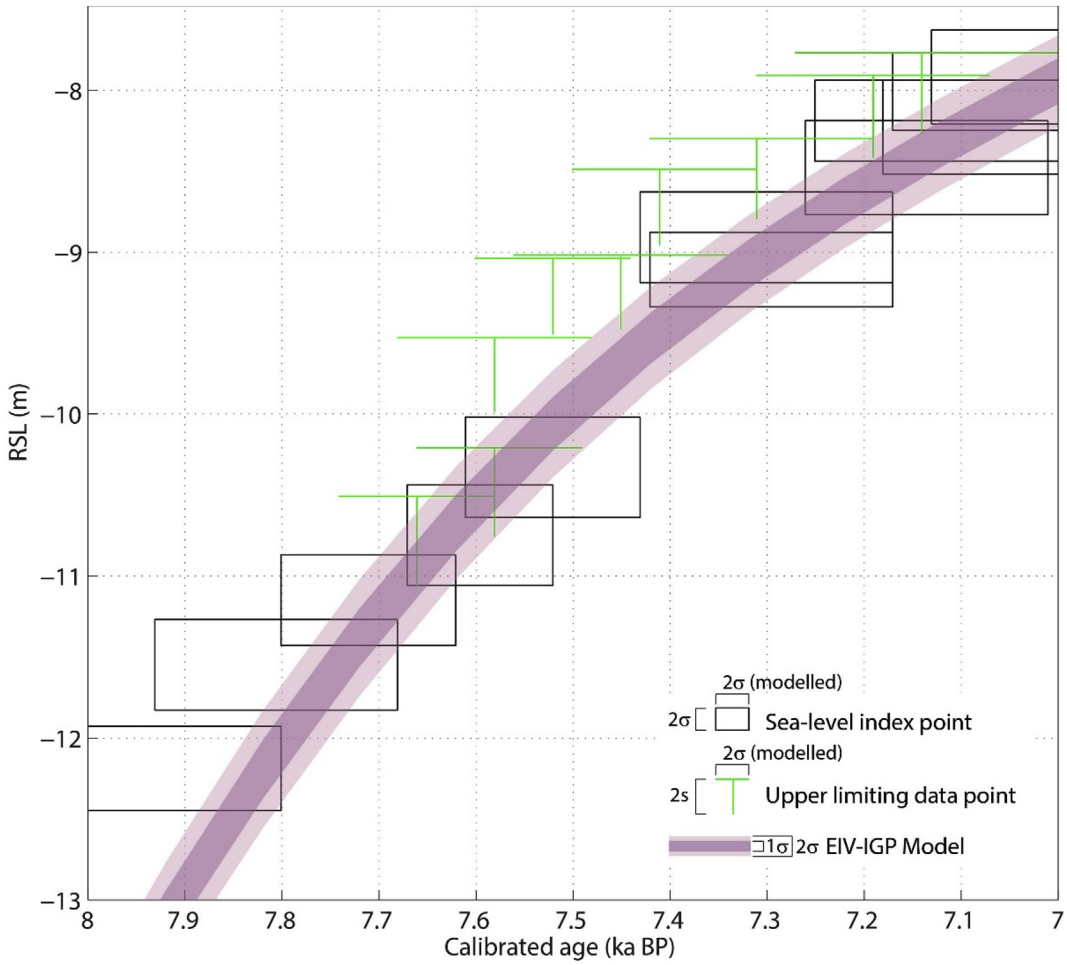

Fig. 8. Plot of the SLIPs and the upper limiting data around the 7.6 ka BP event. A sea-level jump with a magnitude of 4.5 m can be excluded, and if a sea-level jump occurred it would have been small. The confidence intervals were calculated using the model described in Cahill et al. (2015, 2016).

locations, but rather rates of the upstream shifting of a river mouth.

Whereas dating the transgression contact at the top of the basal peat provides for direct SLIP collection and RSLR quantification opportunities, the default for dates of the onset of basal peat formation on valley floors is to consider these upper limiting data points. Although these do not pinpoint past sea levels exactly, the existence of basal peat from a certain moment is an indirect record of RSL prior to drowning in rising estuarine waters. If clusters of dates are collected one may be able to identify and upgrade a portion of the dates to SLIPs (Section 3), a situation that for the RMD palaeovalley applied to the Maasvlakte subarea between 9.0-8.5 ka (Figs. 5 and 6). At that position in the palaeovalley, the basal-peat producing swamps established regionally around 9.2 ka (Vos et al., 2015). For the Po Delta and the associated Adriatic inner shelf a marked transgression phase has been proposed for this time period (Amorosi et al., 2017; Bruno et al., 2017), followed by lower rates of RSLR. Several other studies also describe accelerated SLR around that time, clustering in a 9.6–9.3 ka BP age range (Zong et al., 2009; Amorosi et al., 2013), while Yu et al. (2010) provide a possible source for this acceleration, namely a freshwater outburst from Lake Superior. If such a punctuated transgression history is adopted for the Southern Bight and the RMD too, then the age-clustering of basal peats in the Maasvlakte area would mark the decelerated RSLR phase between the 9.2 and the 8.5–8.2 ka BP accelerations. In turn, this would mean that the palaeovalley floors below −25 m O.D. were transgressed faster (as part of the pre-9.2 ka BP acceleration), than the reach with depths between −25 and −20 m O.D., which could explain the relative scarcity of basal-peat data at greater depths. This would be an analogy to what is observed inland of the 9.2–8.5 basal-peat cluster: between the Maasvlakte and Rotterdam areas, valley floor basal-peat patches from between 8.5–8.2 are rare to absent and instead gyttjaic muds of the same age dominate the Holocene basal organic bed (Cohen, 2005; Hijma and Cohen, 2010; Bos et al., 2012) as a consequence of accelerated RSLR. This way of interpreting replacement of swamp vs. subaqueous muddy organic beds along a transgressive surface is an established practice in sequence stratigraphic interpretations (Bohacs and Suter, 1997; Amorosi et al., 2017) and appears to be of explorative use for sea-level studies too. To confirm such ideas, further work is required to upgrade the resolution of the offshore transgressive record of the Southern Bight of the North Sea.

A welcome first offshore extension of the RMD SLIP record would be data from around 9.5 ka BP, so from before the 9.2 ka BP change of accelerated to decelerated rates of RSLR. Far-field reconstructions suggest the amount of eustatic RSLR between 9.5 and 8.5 ka BP to be approximately 13–15 m (Lambeck et al., 2014). In the south of the Southern Bight an additional 1–3 m of glacio-isostatic subsidence should be considered over that same time (Kiden et al., 2002; Vink et al., 2007), suggesting that the target depth for SLIPs dating to around 9.5 ka BP is to be sought near 36–38 m below O.D (16–18 m below the level of 8.5 ka BP). Indeed, all upper limiting data points plot to the older side of such a linear approximation of

RSLR in the palaeovalley between the RMD and the Rhine-Meuse-Scheldt-Thames confluence zone in the southern most sectors of the North Sea (Fig. 5). Offshore research within the Anglo-Belgian-French continuation of the Rhine-Meuse palaeovalley could resolve the onset of acceleration before 9.2 ka BP, while research closer to the present coast could resolve the deceleration limb following it.

In the GIA-modelling based analysis of far-field data of Lambeck et al. (2014: their Fig. 4), accelerations around 9.2 and 8.5–8.2 ka BP are unresolved. That analysis avoided inclusion of datasets from major Asian deltas and the bases of their inshore transgressive paleovalley fills, because of excess subsidence effects from sediment loading, that would complicate GIA-model iterations that primarily consider ice and water loads. It is important to realise, however, that the additional subsidence term in major delta regions (see e.g. Kuchar et al., 2018) stretches the vertical range from which SLIP series can be accumulated with benefit for resolving punctuated events on top of background RSLR trends. This applies to deltas of the Asian far-field (Mekong Delta: Tamura et al., 2009; Tjallingii et al., 2010; Tjallingii et al., 2014), (Yangtze Delta: Wang et al., 2013), (Pearl delta: Zong et al., 2009), but also to near-field deltas in the U.S. (Li et al., 2012) and in Europe (Hijma and Cohen, 2010; Amorosi et al., 2017).

6. Conclusions

The new sea-level database for the Rhine-Meuse Delta contains 50 SLIPs and 56 upper limiting data points spanning a depth range of −34 to −1.5 m. The SLIPs cover the age-range 8.8–3.0 ka; for the upper limiting data point the age range extends back to 11.5 ka BP. The database has been created by reassessing all existing sea-level data and adding 5 previously unpublished points, hereby specifying the precision and suitability of each point. For the Rhine-Meuse lower delta plain and adjacent offshore area, this involved categorizing the basal-peat samples of various settings and depositional environments that evolved between 11.5 and 3.0 ka BP and subsequently labelling them as either SLIPs or upper limiting data points. We weighed data-point properties such as sampling quality, MSL indicative meaning based on depositional environment and stratigraphic position, palaeotidal changes and age-depth position of an individual sample against nearby samples. Restricting the screening activities to basal-peat samples (95% of the entries in the database), kept compaction-related uncertainties in the SLIP and upper limiting data points small. The age-depth data density and spatial concentration of subsets of dates allowed to perform Bayesian radiocarbon calibration to reduce temporal uncertainty by 25% for the average sample (1σ age uncertainty ≈ 75 cal. yr), when depth position, steady positive sea-level rise tendency and SLIP/non-SLIP judgement are used to assign sequence order.

The protocol-derived positions of the SLIPs are in general agreement with published MSL RSLR curves for the study area from the last decade. The trends and events in the dataset for specific time intervals are:

- Before 8.8 ka: For this time interval, the database consists of data from offshore the RMD. Only offshore data with a contextual relationship with the Rhine-Meuse palaeovalley (floor and shoulders) or the lowermost regions of its main tributaries (Thames, Medway from the English side, Scheldt from the Belgian-Dutch side) were included. Currently, all offshore database entries are upper limiting points, plot below −25 m O.D., and were each collected 40 + years ago. To improve late-Pleistocene to early Holocene records, transgressed basal-peat beds at target depths between 40 and 25 m below modern MSL should be obtained. Until such activities have been undertaken, only the upper bound of RSLR trends before 8.8 ka BP can be estimated, fed with global insights in post-glacial eustasy, regional estimates regarding rates of GIA and tectonic subsidence, and sedimentary geological interpretation of depth-distributions of scattered basal-peat presence.
- 8.8–8 ka BP: the average rate of RSLR during this period was ~10 mm/yr, but the rise was more punctuated (i.e., stepped) in this period than after 8 ka BP. In general, the SLIPs in the database comply to the earlier sea-level reconstruction for this interval by Hijma and Cohen (2010), but has been revised to account for information from new SLIPs and increased insight in the structure of the pre-8.2 ka sea-level jump of which the source is linked to events in the Lake Agassiz-Ojibway region, besides minor differences in database protocol. In the RMD, we now start to resolve a two-phased substructure, with phases starting at 8.44 ± 0.41 ka BP and 8.22 ± 0.65 ka BP and with respective magnitudes of 1.7 ± 0.6 m and 0.2 ± 0.2 m, translating to globally-averaged magnitudes of 2.5 m ± 0.9 m for the first and 0.3 ± 0.3 m for the second phase.
- 8–3 ka BP: In general the SLIPs in the database reproduce the smooth (i.e., non-stepped) MSL reconstruction for this interval by Van de Plassche et al. (2010) and hence the trend of gradually decelerating RSLR, with rates dropping from 9 mm/yr to a 1 mm/yr background value over this period. The deceleration is attributed to a decreasing eustatic contribution and relaxing GIA subsidence. The residual rates attained at 4.5 ka (and maintained into the Common Era) are attributed to residual GIA and tectonic subsidence of the study area as a southerly depocentre in the North Sea Basin. The RMD sea-level database excludes a globally observed RSLR accelleration around 7.6 ka BP to have had a meter-scale magnitude. The maximum magnitude that a step (jump) in sea-level at that time may have had in the RMD is a few decimeters.
- 3.0 ka BP - present: there is an absence of data for this period because we restricted the analysis to sea-level reconstructions based on basal peats. Basal-peat beds have not survived through the youngest millennia, mainly due to human activities in the densely populated RMD plain.

Acknowledgments

This paper is dedicated to the memory of Saskia Jelgersma (1929–2012) and Orson van de Plassche (1947–2009), two pioneering Dutch sea-level researchers who have inspired many researchers around the world. Their data continue to be an important part of the Rhine-Meuse sea-level database presented in this paper. We also acknowledge the efforts of all other researchers whose data have been included into the RMD-database. Two anonymous reviewers and the guest editors are thanked for their thoughtful comments and suggestions. Dr. Niamh Cahill (Maynooth University) is thanked for providing and discussing the results from the EIV-IGP-model. Special thanks to Prof. Judith Verstegen (University of Münster) for commenting on a draft and Marieke Hijma BSc for tipping us on the Blijdorp building pit in Rotterdam: we will never forget. Part of the work by M.P.H. was executed within the programme 'KPP-B&O Kust' of Rijkswaterstaat (Dutch Ministry of Infrastructure and Water Management). The authors acknowledge the PALSEA (a PAGES/INQUA) working group for useful discussions at the 2016 meeting (Oregon, USA).

Appendix A. Supplementary data

Supplementary data associated with this article can be found, in the online version, at https://doi.org/10.1016/j.quascirev.2019.05.001.

References

Amorosi, A., Rossi, V., Vella, C., 2013. Stepwise post-glacial transgression in the Rhône Delta area as revealed by high-resolution core data. Palaeogeogr. Palaeoclimatol. Palaeoecol. 374 (Suppl. C), 314–326. https://doi.org/10.1016/j.palaeo.2013.02.005.

Amorosi, A., et al., 2017. Global sea-level control on local parasequence architecture from the Holocene record of the Po Plain, Italy. Mar. Petrol. Geol. 87 (Suppl. C), 99–111. https://doi.org/10.1016/j.marpetgeo.2017.01.020.

Barber, D.C., et al., 1999. Forcing of the cold event of 8,200 years ago by catastrophic drainage of Laurentide lake. Nature 400, 344–348.

Berendsen, H.J.A., Stouthamer, E., 2000. Late weichselian and Holocene palaeogeography of the rhine-meuse delta, The Netherlands. Palaeogeogr. Palaeoclimatol. Palaeoecol. 161 (3–4), 311–335.

Berendsen, H.J.A., et al., 2007. New groundwater-level rise data from the Rhine-Meuse delta - implications for the reconstruction of Holocene relative mean sea-level rise and differential land-level movements. Neth. J. Geosci. Geol. Mijnb. 86 (4), 333–354.

Bird, M.I., et al., 2007. An inflection in the rate of early mid-Holocene eustatic sea-level rise: a new sea-level curve from Singapore. Estuar. Coast Shelf Sci. 71 (3–4), 523–536.

Blanchon, P., Jones, B., Ford, D.C., 2002. Discovery of a submerged relic reef and shoreline off Grand Cayman: further support for an early Holocene jump in sea level. Sediment. Geol. 147 (3–4), 253–270.

Bohacs, K., Suter, J., 1997. Sequence stratigraphic distribution of coaly rocks: fundamental controls and paralic examples. AAPG (Am. Assoc. Pet. Geol.) Bull. 81 (10), 1612–1639.

Bos, I.J., Busschers, F.S., Hoek, W.Z., 2012. Organic-facies determination: a key for understanding facies distribution in the basal peat layer of the Holocene Rhine-Meuse delta, The Netherlands. Sedimentology 59 (2), 676–703. https://doi.org/10.1111/j.1365-3091.2011.01271.x.

Bridgland, D.R., D'Olier, B., 1995. The pleistocene evolution of the Thames and rhine drainage systems in the Southern North Sea Basin. Geol. Soc. Lond. Special Publ. 96 (1), 27–45.

Broekman, R., Kösters, A., 2010. Nauwkeurig NAP-hoogten meten: GPS of waterpassen? Geo-Info 10 (2), 26.

Bronk Ramsey, C., 2009. Bayesian analysis of radiocarbon dates. Radiocarbon 51 (1), 337–360.

Bruno, L., et al., 2017. Early Holocene transgressive palaeogeography in the Po coastal plain (northern Italy). Sedimentology 64 (7), 1792–1816. https://doi.org/10.1111/sed.12374.

Busschers, F.S., et al., 2007. Late Pleistocene evolution of the Rhine-Meuse system in the southern North Sea basin: imprints of climate change, sea-level oscillation and glacio-isostacy. Quat. Sci. Rev. 26 (25-28), 3216–3248.

Cahill, N., Kemp, A.C., Horton, B.P., Parnell, A.C., 2015. Modeling sea-level change using errors-in-variables integrated Gaussian processes. Ann. Appl. Stat. 9 (2), 547–571. https://doi.org/10.1214/15-AOAS824.

Cahill, N., Kemp, A.C., Horton, B.P., Parnell, A.C., 2016. A Bayesian hierarchical model for reconstructing relative sea level: from raw data to rates of change. Clim. Past 12 (2), 525–542. https://doi.org/10.5194/cp-12-525-2016.

Carlson, A.E., et al., 2008. Rapid early Holocene deglaciation of the Laurentide ice sheet. Nat. Geosci. 1 (9), 620–624.

Carlson, A.E., Clark, P.U., 2012. Ice sheet sources of sea level rise and freshwater discharge during the last deglaciation. Rev. Geophys. 50 (RG4007) https://doi.org/10.1029/2011RG000371.

Clerkx, A.P.P.M., et al., 1994. Broekbossen van Nederland, IBN-rapport 096, Instituut voor Bos- en of macrofossils from that particular level yields consistent. Natuuronderzoek/Staring Centrum, Wageningen.

Cohen, K.M., 2005. 3D geostatistical interpolation and geological interpolation of palaeo-groundwaterrise within the coastal prism in The Netherlands. In: Giosan, L., Bhattacharaya, J.P. (Eds.), River Deltas: Concepts, Models, and Examples. SEPM (Society for Sedimentary Geology), Tulsa, Oklahoma, USA, pp. 341–364.

Cohen, K.M., Stouthamer, E., Pierik, H.J., Geurts, A., 2012. Digitaal Basisbestand Paleogeografie van de Rijn-Maas Delta/Rhine-Meuse Delta Studies' Digital Basemap for Delta Evolution and Palaeogeography. Dept. Physical Geography. Utrecht University, Digital Dataset.

Cohen, K.M., et al., 2017. Mapping buried Holocene landscapes : past lowland environments, palaeoDEMs and preservation in GIS. In: Lauwerier, R.C.G.M., et al. (Eds.), Knowledge for Informed Choices. Nederlandse Archeologische Rapporten (NAR). Rijksdienst Voor Cultureel Erfgoed, Amersfoort, The Netherlands, pp. 73–95.

Conradsen, K., Heier-Nielsen, S., 1995. Holocene paleoceanography and paleoenvironments of the skagerrak-kattegat, scandinavia. Paleoceanography 10 (4), 801–813.

Daubois, V., Roy, M., Veillette, J.J., Ménard, M., 2015. The drainage of Lake Ojibway in glaciolacustrine sediments of northern Ontario and Quebec, Canada. Boreas 44 (2), 305–318. https://doi.org/10.1111/bor.12101.

De Groot, T.A.M., Westerhoff, W.E., Bosch, J.H.A., 1996. Sea-level rise during the last 2000 years as recorded on the Frisian Island (The Netherlands). In: Beets, D.J., Fischer, M.M., De Gans, W. (Eds.), Coastal Studies on the Holocene of the Netherlands. Med. Rijks. Geol. Dienst. Rijks Geologische Dienst, Haarlem, pp. 69–78.

De Haas, T., et al., 2018. Holocene evolution of tidal systems in The Netherlands: effects of rivers, coastal boundary conditions, eco-engineering species, inherited relief and human interference. Earth Sci. Rev. 177, 139–163. https://doi.org/10.1016/j.earscirev.2017.10.006.

De Vries, J.J., 1974. Groundwater Flow Systems and Stream Nets in The Netherlands. Ph.D.-thesis. Free University of Amsterdam, 226 pp.

Delibrias, G., Guillier, M., Labeyrie, J., 1974. Gif natural radiocarbon measurements VIII. Radiocarbon 16 (1), 15–94.

Den Held, A., Schmitz, M., Van Wirdum, G., 1992. Types of terrestrializing fen vegetation in The Netherlands. In: Verhoeven, J.T.A. (Ed.), Fens and Bogs in the Netherlands: Vegetation, History, Nutrient Dynamics and Conservation. Geobotany. Kluwer Academics Publishers, Dordrecht, pp. 237–321.

Denys, L., Baeteman, C., 1995. Holocene evolution of relative sea-level and local mean high water spring tides in Belgium - a first assessment. Mar. Geol. 124, 1–19.

Devoy, R.J.N., 1979. Flandrian sea level changes and vegetational history of the lower Thames estuary. Phil. Trans. Roy. Soc. Lond. B Biol. Sci. 285, 355–407.

Domínguez-Villar, D., et al., 2009. Oxygen isotope precipitation anomaly in the North Atlantic region during the 8.2 ka event. Geology 37 (12), 1095–1098. https://doi.org/10.1130/G30393A.1.

Ellison, C.R.W., Chapman, M.R., Hall, I.R., 2006. Surface and deep ocean interactions during the cold climate event 8200 years ago. Science 312 (5782), 1929–1932.

Hijma, M.P., Cohen, K.M., Hoffmann, G., Van der Spek, A.J.F., Stouthamer, E., 2009. From river valley to estuary: the evolution of the Rhine mouth in the early to middle Holocene (western Netherlands, Rhine-Meuse delta). Neth. J. Geosci. Geol. Mijnb. 88 (1), 13–53.

Hijma, M.P., Cohen, K.M., 2010. Timing and magnitude of the sea-level jump preluding the 8200 yr event. Geology 38 (3), 275–278.

Hijma, M.P., Van der Spek, A.J.F., Van Heteren, S., 2010. Development of a mid-Holocene estuarine basin, Rhine-Meuse mouth area, offshore The Netherlands. Mar. Geol. 271 (3–4), 198–211.

Hijma, M.P., Cohen, K.M., 2011a. Holocene transgression of the Rhine river mouth area, The Netherlands/Southern North Sea: palaeogeography and sequence stratigraphy. Sedimentology 58 (6), 1453–1485.

Hijma, M.P., Cohen, K.M., 2011b. Comment on: mid-Holocene water-level changes in the lower Rhine-Meuse delta (western Netherlands): implications for the reconstruction of relative mean sea-level rise, palaeoriver-gradients and coastal evolution by Van de Plassche et al. (2010). Neth. J. Geosci. Geol. Mijnb. 90 (1), 51–54.

Hijma, M.P., Cohen, K.M., Roebroeks, W., Westerhoff, W.E., Busschers, F.S., 2012. Pleistocene Rhine-Thames landscapes: geological background for hominin occupation of the southern North Sea region. J. Quat. Sci. 27 (1), 17–39. https://doi.org/10.1002/jqs.1549.

Hijma, M.P., et al., 2015. A protocol for a geological sea-level database. In: Shennan, I., Long, A.J., Horton, B.P. (Eds.), Handbook of Sea-Level Research. Wiley Blackwell, pp. 536–553.

Jelgersma, S., 1961. Holocene sea-level changes in The Netherlands. Meded. Geol. Sticht. 7, 1–101.

Jelgersma, S., 1966. Sea-level changes during the last 10.000 years. In: Proceedings of the International Symposium on World Climate 8000-0 BC. Royal Meteorological Society, London, pp. 54–71.

Jelgersma, S., 1979. Sea-level changes in the North Sea basin. In: Oele, E., Schüttenhelm, R., Wiggers, A.J. (Eds.), Acta Univ. Ups. Symp. Univ. Ups, vol. 2. Annum Quingentesimum Celebrantis, pp. 233–248.

Jiang, H., Björck, S., Knudsen, K.L., 1997. A palaeoclimatic and palaeoceanographic record of the last 11 000 14C years from the Skagerrak-Kattegat, northeastern Atlantic margin. Holocene 7 (3), 301–310.

Kendall, R.A., Mitrovica, J.X., Milne, G.A., Törnqvist, T.E., Li, Y., 2008. The sea-level fingerprint of the 8.2 ka climate event. Geology 36 (5), 423–426.

Kiden, P., 1995. Holocene relative sea-level change and crustal movement in the southwestern Netherlands. Mar. Geol. 124, 21–41.

Kiden, P., Denys, L., Johnston, P., 2002. Late Quaternary sea-level change and isostatic and tectonic land movement along the Belgian-Dutch North Sea coast: geological data and model results. J. Quat. Sci. 17, 535–546.

Kirby, R., Oele, E., 1975. The geological history of the sandettie-fairy bank area, Southern North sea. Phil. Trans. Roy. Soc. Lond. Math. Phys. Sci. 279 (1288), 257–267.

Kooi, H., Johnston, P., Lambeck, K., Smither, C., Ronald, M., 1998. Geological causes of recent (~100 yr) vertical land movement in The Netherlands. Tectonophysics 299 (4), 297–316.

Koster, K., Stafleu, J., Cohen, K.M., 2017. Generic 3D interpolation of Holocene base-level rise and provision of accommodation space, developed for The Netherlands coastal plain and infilled palaeovalleys. Basin Res. 29 (6), 775–797. https://doi.org/10.1111/bre.12202.

Kuchar, J., et al., 2018. The influence of sediment isostatic adjustment on sea-level change and land motion along the US gulf coast. J. Geophys. Res.: Solid Earth 123 (1), 780–796. https://doi.org/10.1002/2017JB014695.

Lajeunesse, P., St-Onge, G., 2008. The subglacial origin of the Lake Agassiz-Ojibway final outburst flood. Nat. Geosci. 1 (3), 184–188.

Lambeck, K., 1995. Late devensian and Holocene shorelines of the British isles and north sea from models of glacio-hydro-isostatic rebound. J. Geol. Soc. 152, 437–448.

Lambeck, K., Rouby, H., Purcell, A., Sun, Y., Sambridge, M., 2014. Sea level and global

ice volumes from the last glacial maximum to the Holocene. Proc. Natl. Acad. Sci. Unit. States Am. 111 (43), 15296–15303. https://doi.org/10.1073/pnas.1411762111.
Lawrence, T., Long, A.J., Gehrels, W.R., Jackson, L.P., Smith, D.E., 2016. Relative sea-level data from southwest Scotland constrain meltwater-driven sea-level jumps prior to the 8.2 kyr BP event. Quat. Sci. Rev. 151, 292–308. https://doi.org/10.1016/j.quascirev.2016.06.013.
Lewis, C.F.M., Miller, A.A.L., Levac, E., Piper, D.J.W., Sonnichsen, G.V., 2012. Lake Agassiz outburst age and routing by Labrador Current and the 8.2 cal ka cold event. Commemorative Vol. Honour Jim Teller 260 (0), 83–97. https://doi.org/10.1016/j.quaint.2011.08.023.
Li, Y.-X., Törnqvist, T.E., Nevitt, J.M., Kohl, B., 2012. Synchronizing a sea-level jump, final Lake Agassiz drainage, and abrupt cooling 8200 years ago. Earth Planet. Sci. Lett. 315–316, 41–50. https://doi.org/10.1016/j.epsl.2011.05.034.
Louwe Kooijmans, L.P., 1974. The Rhine/Meuse Delta: Four Studies on its Prehistoric Occupation and Holocene Geology. Ph.D.-thesis. Leiden University, Leiden.
Louwe Kooijmans, L.P., Van den Broeke, P.W., Fokkens, H., Van Gijn, A.L., 2005. Prehistory of the Netherlands, vol. 2. Amsterdam University Press, Amsterdam.
Meijles, E.W., et al., 2018. Holocene relative mean sea-level changes in the Wadden Sea area, northern Netherlands. J. Quat. Sci. 0 (0) https://doi.org/10.1002/jqs.3068.
Morzadec-Kerfourn, M.T., Delibrias, G., 1972. Analyses polliniques et datations radiocarbone des sediments quaternaires preleves en Manche centrale et orientale. Memoires du Bureau de Recherche Geologique et Miniere 79, 160–165.
Nelson, A.R., Shennan, I., Long, A.J., 1996. Identifying coseismic subsidence in tidal-wetland stratigraphic sequences at the Cascadia subduction zone of western North America. J. Geophys. Res. B: Solid Earth 101 (3), 6115–6135. https://doi.org/10.1029/95JB01051.
Peeters, J., et al., 2018. Preservation of last interglacial and Holocene transgressive systems tracts in The Netherlands and its applicability as a North Sea basin reservoir analogue. Earth Sci. Rev. https://doi.org/10.1016/j.earscirev.2018.10.010.
Peltier, W.R., Argus, D.F., Drummond, R., 2015. Space geodesy constrains ice age terminal deglaciation: the global ICE-6G_C (VM5a) model. J. Geophys. Res.: Solid Earth 120 (1), 450–487. https://doi.org/10.1002/2014JB011176.
Reimer, P.J., et al., 2013. IntCal13 and Marine13 radiocarbon age calibration curves 0-50,000 yr cal BP. Radiocarbon 55, 1869–1887.
Roep, T.B., Beets, D.J., 1988. Sea level rise and paleotidal levels from sedimentary structures in the coastal barriers in the western Netherlands since 5600 BP. Geol. Mijnb. 67, 53–60.
Roy, M., et al., 2011. Insights on the events surrounding the final drainage of Lake Ojibway based on James Bay stratigraphic sequences. Quat. Sci. Rev. 30 (5), 682–692. https://doi.org/10.1016/j.quascirev.2010.12.008.
Shennan, I., et al., 2000. Holocene isostasy and relative sea-level changes on the east coast of England. Geol. Soc. Lond. Spec. Publ. 166 (1), 275–298. https://doi.org/10.1144/gsl.sp.2000.166.01.14.
Shennan, I., Long, A.J., Horton, B.P. (Eds.), 2015. Handbook of Sea-Level Research. Wiley/AGU, 600 pp.
Shennan, I., Bradley, S.L., Edwards, R., 2018. Relative sea-level changes and crustal movements in britain and Ireland since the last glacial maximum. Quat. Sci. Rev. 188, 143–159. https://doi.org/10.1016/j.quascirev.2018.03.031.
Slupik, A.A., et al., 2014. The role of a proto-Schelde River in the genesis of the southwestern Netherlands, inferred from the Quaternary successions and fossils in Moriaanshoofd Borehole (Zeeland, The Netherlands). Neth. J. Geosci. Geol. Mijnb. 92 (1), 69–86. https://doi.org/10.1017/S0016774600000299.
Stouthamer, E., Berendsen, H.J.A., 2000. Factors controlling the Holocene avulsion history of the Rhine-Meuse delta (The Netherlands). J. Sediment. Res. 70 (5), 1051–1064.
Tamura, T., et al., 2009. Initiation of the Mekong River delta at 8 ka: evidence from the sedimentary succession in the Cambodian lowland. Quat. Sci. Rev. 28 (3–4), 327–344. https://doi.org/10.1016/j.quascirev.2008.10.010.
Tjallingii, R., Stattegger, K., Wetzel, A., Van Phach, P., 2010. Infilling and flooding of the Mekong River incised valley during deglacial sea-level rise. Quat. Sci. Rev. 29 (11), 1432–1444. https://doi.org/10.1016/j.quascirev.2010.02.022.
Tjallingii, R., Stattegger, K., Stocchi, P., Saito, Y., Wetzel, A., 2014. Rapid flooding of the southern Vietnam shelf during the early to mid-Holocene. J. Quat. Sci. 29 (6), 581–588. https://doi.org/10.1002/jqs.2731.
Törnqvist, T.E., van Ree, M.H.M., van 't Veer, R., van Geel, B., 1998. Improving methodology for high-resolution reconstruction of sea-level rise and neotectonics by paleoecological analysis and AMS ^{14}C dating of basal peats. Quat. Res. 49 (1), 72–85.
Törnqvist, T.E., et al., 2004. Deciphering Holocene sea-level history on the U.S. Gulf Coast: a high-resolution record from the Mississippi Delta. Geol. Soc. Am. Bull. 116 (7), 1026–1039.
Törnqvist, T.E., Hijma, M.P., 2012. Links between early Holocene ice-sheet decay, sea-level rise and abrupt climate change. Nat. Geosci. 5, 601–606. https://doi.org/10.1038/NGEO1536.
Törnqvist, T.E., Rosenheim, B.E., Hu, P., Fernandez, A.B., 2015. Radiocarbon dating and calibration. In: Shennan, I., Long, A.J., Horton, B.P. (Eds.), Handbook of Sea-Level Research. Wiley Blackwell, pp. 349–360.
Uehara, K., Scourse, J.D., Horsburgh, K.J., Lambeck, K., Purcell, A.P., 2006. Tidal evolution of the northwest European shelf areas from the Last Glacial Maximum to the present. J. Geophys. Res. 111. C09025-C09025.
Van Asselen, S., Cohen, K.M., Stouthamer, E., 2017. The impact of avulsion on groundwater level and peat formation in delta floodbasins during the middle-Holocene transgression in the Rhine-Meuse delta, The Netherlands. Holocene 27 (11), 1694–1706. https://doi.org/10.1177/0959683617702224.
Van de Plassche, O., 1980. Compaction and other sources of error in obtaining sea-level data: some results and consequences. Eiszeitalt. Ggw. 30, 171–181.
Van de Plassche, O., 1982. Sea-level Change and Water-Level Movements in The Netherlands during the Holocene. Ph.D.-thesis. Vrije Universiteit, Amsterdam.
Van de Plassche, O., 1986. Introduction. In: Van de Plassche, O. (Ed.), Sea-level Research: a Manual for the Collection and Evaluation of Data. Geobooks, Norwich, pp. 1–26.
Van de Plassche, O., Roep, T.B., 1989. Sea-level changes in The Netherlands during the last 6500 years: basal peat vs. coastal barrier data. In: Scott, D.B., Pirazzoli, P.A., Honig, C.A. (Eds.), Late Quaternary Sea-Level Correlation and Applications. Kluwer, Dordrecht, pp. 41–56.
Van de Plassche, O., 1995. Evolution of the intra-coastal tidal range in the Rhine-Meuse delta and Flevo Lagoon, 5700-3000 yrs cal B.C. Mar. Geol. 124 (1–4), 113–128.
Van de Plassche, O., Bohncke, S.J.P., Makaske, B., Van der Plicht, J., 2005. Water-level changes in the Flevo area, central Netherlands (5300-1500 BC): implications for relative mean sea-level rise in the Western Netherlands. Quat. Int. 133–134, 77–93.
Van de Plassche, O., Makaske, B., Hoek, W.Z., Konert, M., Van der Plicht, J., 2010. Mid-Holocene water-level changes in the lower Rhine-Meuse delta (western Netherlands): implications for the reconstruction of relative mean sea-level rise, palaeoriver-gradients and coastal evolution. Neth. J. Geosci. Geol. Mijnb. 89 (1), 3–20.
Van der Molen, J., Van Dijck, B., 2000. The evolution of the Dutch and Belgian coasts and the role of sand supply from the North Sea. Glob. Planet. Chang. 27 (1–4), 223–244.
Van der Molen, J., De Swart, H.E., 2001. Holocene tidal conditions and tide-induced sand transport in the southern North Sea. J. Geophys. Res. C 106 (C5), 9339–9362.
Van der Woude, J.D., 1984. The fluviolagoonal palaeoenvironment in the Rhine/Meuse deltaic plain. Sedimentology 31 (3), 395–400.
Van der Zon, N., 2013. Kwaliteitsdocument AHN2, Rijkswaterstaat Data-ICT-Dienst. Servicedesk Data, 32 pp.
Van Dijk, G.J., Berendsen, H.J.A., Roeleveld, W., 1991. Holocene water level development in The Netherlands' river area; implications for sea-level reconstruction. Geol. Mijnb. 70 (4), 311–326.
Van Heteren, S., Van der Spek, A.J.F., De Groot, T.A.M., 2002. Architecture of a Preserved Holocene Tidal Complex Offshore the Rhine-Meuse Mouth, the Netherlands. Netherlands Institute of Applied Geoscience TNO - National Geological Survey, 40 pp.
Van Veen, J., Van, d.S., Stive, M.J., Zitman, T., 2005. Ebb and flood channel systems in The Netherlands tidal waters. J. Coast. Res. 21 (6), 1107–1120.
Vermeersen, B.L.A., et al., 2018. sea-Level change in the Dutch wadden sea. Neth. J. Geosci. 97 (3), 79–127. https://doi.org/10.1017/njg.2018.7.
Vink, A., Steffen, H., Reinhardt, L., Kaufmann, G., 2007. Holocene relative sea-level change, isostatic subsidence and the radial viscosity structure of the mantle of northwest Europe (Belgium, The Netherlands, Germany, southern North Sea). Quat. Sci. Rev. 26 (25–28), 3249–3275.
Vis, G.-J., et al., 2015. Paleogeography. In: Shennan, I., Long, A.J., Horton, B.P. (Eds.), Handbook of Sea-Level Research. Wiley Blackwell, pp. 514–535.
Vogel, J.C., Waterbolk, H.T., 1963. Groningen radiocarbon dates IV. Radiocarbon 5 (1), 163–202.
Vos, P.C., 1992. Toelichting kaartblad 43/49 West en 49 Oost-Concept toelichting 43/49 West: Holocene deel (In Dutch), Rijks Geologische Dienst, Dienstrapport 1454, Haarlem, 41 pp.
Vos, P.C., Bunnik, F.P.M., Cremer, H., Hennekman, F.M., 2010. Paleolandschappelijk onderzoek Papegaaienbek en Kop van Beer (In Dutch), Deltares report 1201910-000-BGS-000187.
Vos, P.C., Bazelmans, J., Weerts, H.J.T., Van der Meulen, M.J., 2011. Atlas Van Nederland in Het Holoceen. RCE, TNO en Deltares, 94 pp.
Vos, P.C., 2013. Geologisch en paleolandschappelijk onderzoek Yangtzehaven (Maasvlakte, Rotterdam) (In Dutch), Deltares report 1206788-000-BGS-000187.
Vos, P.C., Cohen, K.M., 2014. Landschape genesis and palaeogeography. In: Moree, J.M., Sier, M.M. (Eds.), Interdisciplinary Archaeological Research Programme Maasvlakte 2, vol. 566. BOOR Rotterdam, BOORrapporten, Rotterdam, pp. 63–146.
Vos, P.C., Bunnik, F.P.M., Cohen, K.M., Cremer, H., 2015. A staged geogenetic approach to underwater archaeological prospection in the Port of Rotterdam (Yangtzehaven, Maasvlakte, The Netherlands): a geological and palaeoenvironmental case study for local mapping of Mesolithic lowland landscapes. Quat. Int. 367, 4–31. https://doi.org/10.1016/j.quaint.2014.11.056.
Wang, Z., et al., 2013. Early to mid-Holocene rapid sea-level rise and coastal response on the southern Yangtze delta plain, China. J. Quat. Sci. 28, 659–672.
Ward, S.L., Neill, S.P., Scourse, J.D., Bradley, S.L., Uehara, K., 2016. Sensitivity of palaeotidal models of the northwest European shelf seas to glacial isostatic adjustment since the Last Glacial Maximum. Quat. Sci. Rev. 151, 198–211. https://doi.org/10.1016/j.quascirev.2016.08.034.
Yu, S.-Y., Berglund, B.E., Sandgren, P., Lambeck, K., 2007. Evidence for a rapid sea-level rise 7600 yr ago. Geology 35 (10), 891–894.

Yu, S.-Y., et al., 2010. Freshwater outburst from Lake superior as a trigger for the cold event 9300 Years ago. Science 328 (5983), 1262–1266.
Yu, S.-Y., Törnqvist, T.E., Hu, P., 2012. Quantifying Holocene lithospheric subsidence rates underneath the Mississippi Delta. Earth Planet. Sci. Lett. 331–332 (0), 21–30. https://doi.org/10.1016/j.epsl.2012.02.021.
Zong, Y., Yim, W.W.S., Yu, F., Huang, G., 2009. Late Quaternary environmental changes in the Pearl River mouth region, China. Quat. Int. 206 (1), 35–45. https://doi.org/10.1016/j.quaint.2008.10.012.
Zonneveld, I.S., 1960. De Brabantse Biesbosch. Een studie van bodem en vegetatie van een zoetwatergetijdendelta. Ph.D.-thesis. Wageningen Universiteit, Wageningen, The Netherlands.